A Novel Puncture Method for Determining Plant Stem Morphology and Lodging Resistance

A Thesis

Presented in Partial Fulfillment of the Requirements for the

Degree of Master of Science

with a

Major in Mechanical Engineering

in the

College of Graduate Studies

University of Idaho

by

Will Seegmiller

Major Professor: Daniel Robertson, Ph.D., P.E.

Committee Members: Michael Maughan, Ph.D., P.E.; Matthew Swenson, Ph.D., P.E.

Department Administrator: Steven Beyerlein, Ph.D., P.E.

August 2020

Authorization to Submit Thesis

This thesis of Will Seegmiller, submitted for the degree of Master of Science with a Major in Mechanical Engineering and titled "A Novel Puncture Method for Determining Plant Stem Morphology and Lodging Resistance," has been reviewed in final form. Permission, as indicated by the signatures and dates below, is now granted to submit final copies to the College of Graduate Studies for approval.

Major Professor: ____ Date: ______________

Daniel Robertson, Ph.D., P.E.

Committee Members: ____ Date: ______________

Matthew Swenson, Ph.D., P.E.

____ Date: ______________

Michael Maughan, Ph.D., P.E.

Department

Administrator: ____ Date: ______________

Steven Beyerlein, Ph.D., P.E.

Abstract

Background

Maize (Zea Mays L.) is one of the most extensively grown crops in the world. Due to lodging, or plant destruction caused by high wind and rain, 5% to 15% of the annual global crop is lost. Developing maize hybrids that exhibit high lodging resistance could increase food security and decrease the risk of crop loss. A new method of predicting stem lodging resistance is presented in this thesis.

Results

A novel rind puncture technique was used to obtain measurements of rind thickness and diameter for samples of poison hemlock (Conium maculatum) that were highly correlated with caliper measurements and photographic image analysis measurements. Higher sample throughput was demonstrated by the novel rind puncture technique than by caliper measurements and image analysis techniques. The data generated by the novel puncture method was used to calculate an index quantity (the Integrated Puncture Score) that was highly correlated with stem failure load in maize.

Conclusions

The novel rind puncture technique shows promise as a high throughput method for determining rind thickness and diameter. The technique is an excellent candidate for direct implementation in the field. The Integrated Puncture Score shows promise as a breeding metric for producing lodging resistant maize hybrids.

Acknowledgements

I would like to acknowledge the tremendous assistance and guidance provided by Dr. Daniel Robertson throughout the entirety of my time in graduate school. Invaluable in the preparation of this document were Dr. Michael Maughan, and Dr. Matthew Swenson. Yusuf Oduntan kindly provided the closeup image of the maize cross section in this thesis. I thank Jadzia Graves, Taylor Spence, and Kate Seegmiller for their assistance in collecting data, establishing procedures, and analyzing results. I would like to thank Dr. Daniel Robertson, Dr. Christopher Stubbs, Dr. Douglas Cook, and Dr. Christopher McMahan for their invaluable contributions to the work presented in this thesis.

Dedication

I gratefully dedicate this work to my lovely wife and to my parents. All my successes are owed to their love and care.

Table of Contents

List of Figures

List of Tables

Chapter 1 – Introduction

1.1 Introduction

This thesis details a series of experiments performed to identify and validate a novel breeding metric for maize and other large grains. This novel metric would allow plant scientists and breeders to improve the lodging (i.e. stalk breakage due to high wind and heavy rain) resistance of vulnerable crops by improving their bending strength. This chapter presents the motivation for the study, properties and characteristics of maize plants, and the findings of relevant prior studies.

1.2 Study motivation

Maize is a major cereal crop that is grown widely around the world. In the 2018/2019 growing season, over 360 million metric tons of maize was grown in the U.S. alone [1]. About 380 million square kilometers of land in the U.S. (about 2.5% of total land area in the U.S.) is dedicated to producing maize [2]. Annual yield losses due to lodging range from 5 to 20% worldwide [3]. For such a widely cultivated crop, this represents a serious loss and can disrupt global food security [4]. Mitigating this annual loss could represent a substantial benefit for the world from an economic and humanitarian standpoint. Approximately 90 percent of commercially grown maize in the U.S. is dent corn [1]. Dent corn is allowed to dry in the field before harvest. Stalks that lodge after drying are said to undergo late season stalk lodging. This work will focus specifically on late season stalk lodging in dent corn varieties.

1.3 A description of maize

Description of maize anatomy

Maize stems consist of roughly 4 to 8 sections, called internodes. These sections are separated by boundary regions of very dense and hard tissue, called nodes. Internodes and nodes exhibit an elliptical cross section in the lower portion of the stem. Internodes that support ears of grain have a less regular profile. Nodes regularly exhibit a larger circumference than the internodes they separate.

Stalks taper in circumference, becoming gradually narrower from base to tip. Figure 1.1 visualizes the typical profile of a maize stem.

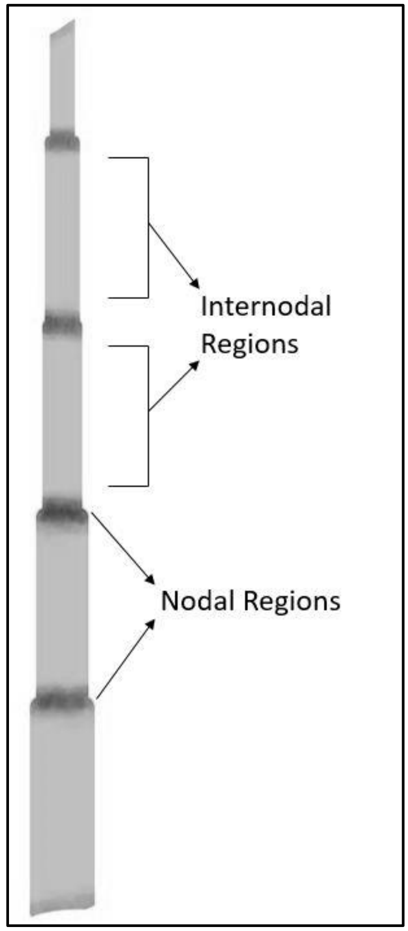

Figure 1.1: Profile of a typical maize stem

Types of tissues present in maize stalks

Three primary tissues are present in maize stems: rind, pith, and vascular bundles (see Figure 1.2). Rind tissue is composed primarily of sclerenchyma cells. Rind tissue has a high cellulose and lignin content, giving it its rigid woody texture in late season maize stems. The rind forms the outermost protective layer of the stem. The pith is composed of largely of parenchyma cells and fills the center of the stem. In late season maize, the pith takes on a foamy, spongy texture. Vascular tissue bundles, composed of xylem and phloem cells, populate the rind in high density and the pith in lower density with a steep density gradient in the region forming the rind-pith transition region [5-8].

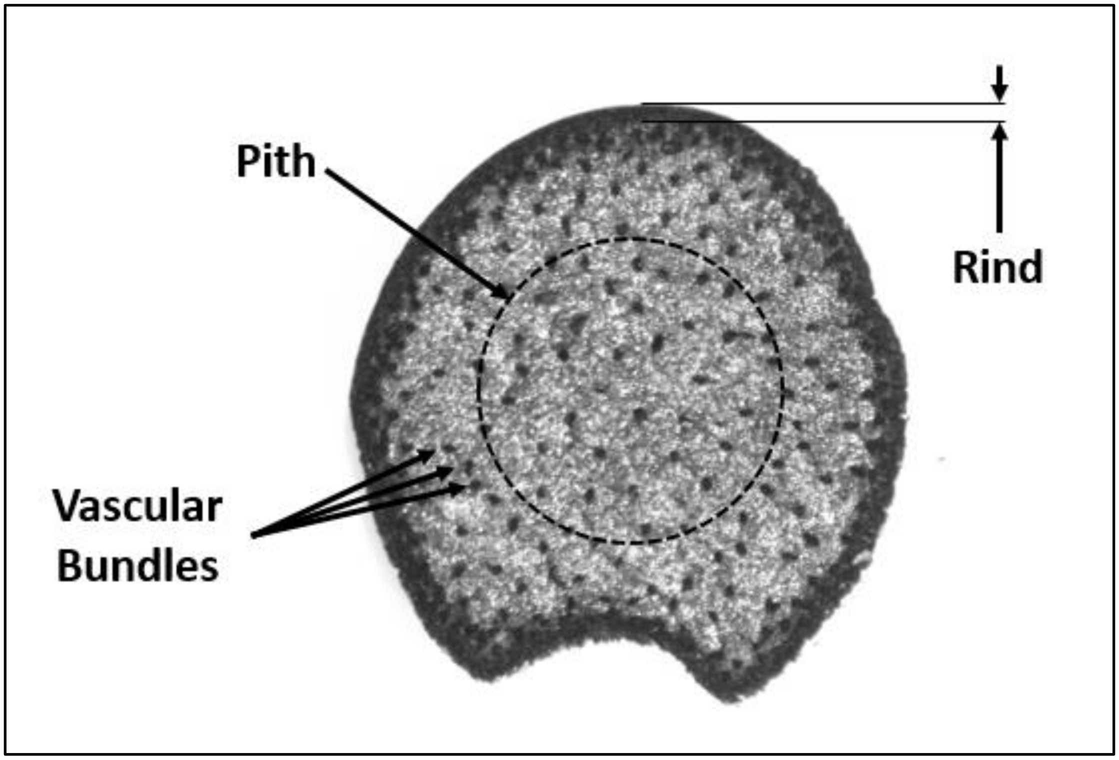

Figure 1.2: A typical maize stem section with different tissue regions indicated. The internode shown was sectioned using a six inch silver notched diamond trimsaw blade (800 RPM). The cross section was stained with Alcian Blue and Safranin O.

Mechanical role of the rind

The rind makes up the outermost layer of a maize stem. The rind is typically between 1 and 3 millimeters in thickness in fully mature stems. The rind is responsible for taking up most of the compressive and bending stresses the stem experiences and is the primary load bearing tissue of the stem.

Mechanical role of the pith

The pith does little to directly increase stalk lodging resistance by itself but does have a key mechanical role. By acting as a mechanical brace and resisting the ovalization of the internode due to bending loads, the pith helps the internode to withstand buckling [9-11]. The pith is less effective at performing this function if there are macrovoids in the tissue matrix. Removing the transverse bracing structures (i.e. tissues mechanically analogous to the pith in maize) in grass stems results in the stems bending strength being reduced by up to 20% [9]. Similar results were obtained in studies of composite foam filled tubes made from engineering materials [12,13].

Mechanical role of the vascular bundles

Within a maize stem, the primary purpose of vascular bundles is not mechanical. However, the vascular bundles do strengthen the stem in tension, and several studies have determined that the quantity of vascular bundles is positively correlated with various mechanical properties of stalk crops [14-16].

Mechanical role of nodes

Nodes are extremely tough, rigid sections on a maize stalk. They are denser and larger in circumference than inter nodal tissues to help the stalk handle bending stresses. They also provide transverse reinforcement to prevent compressive buckling [17].

1.4 Prior studies of lodging resistance in maize

Predominant failure modes in maize

Three failure predominant modes (i.e. snapping, splitting, and creasing) have been identified in late season lodged maize, with creasing failures occurring in over 90% of the studied samples. The creasing is a result of brazier buckling (ovalization of the transverse area of a narrow beam under bending loads). In naturally lodged maize stems the plant typically fails approximately 1 cm above a node [18].

Impact of stress concentrators in maize

The consistent failure location and failure type in lodged maize stems is likely due to geometric and material stress concentrators inherent in stems. In particular, failure typically occurs in or near the intercalary meristem. This region exhibits a rough, irregular surface [19], and the stalk also exhibits rapid changes in diameter in this region. These features commonly appear in many maize varieties and planting/growing conditions [17].

Determining mechanical properties and lodging resistance

An ideal tool for determining lodging resistance would possess the following traits: A quick and simple test procedure, an accurate assessment of stem strength (i.e. typically bending strength), not being confounded by environmental factors (i.e. to allow the test to be used in a wide variety of environmental settings), and minimizing damage to the stalk (i.e. allowing repeat tests over time of the same stalk) [20,21].

The most common tests to quantify the lodging resistance of maize stems include counting the number of lodged plants at harvest, three-point bending tests, and rind penetration tests. The paragraphs below discuss these tests.

Discussion of historical lodging counts

Historically, the propensity of any variety of maize to lodge has been measured by a visual count of lodged stalks at harvest. This method is simple yet unreliable for determining the lodging resistance of a breed as it can be confounded by a variety of environmental factors such as extreme or unseasonal weather, disease, or pest damage[3]. Therefore, many data points acquired over several years in various locations are required to determine the relative lodging resistance of different maize varieties. None the less, lodging counts remain a primary tool used to quantify lodging resistance today [22,23].

Discussion of three-point bending tests

Three-point bending tests have been used in various studies to study stem bending strength and lodging resistance [24-28]. Robertson et al. emphasized maximizing the span length of maize stems in three-point bending tests to accurately measure the bulk properties of the stem. They also emphasized loading the stem exclusively on nodes in three-point bending tests. If an internode is loaded, it will undergo local failure at the loading point and cause stem fracture at lower loads than if the stem is loaded at the nodes [17]. While three-point bending tests are effective at measuring the bending strength of maize stems, they typically require a laboratory setting. This makes them unsuitable for high throughput field testing. In addition, three-point bending tests are destructive to the stem, complicating follow up testing.

Discussion of rind penetration tests

A rind penetration test is conducted by pushing a narrow probe into the rind of a maize stem and recording the resistance forces experienced by the probe. Twumasi-Afriyie and Hunter emphasized that rind penetrance tests are simple, quick, and non-fatal, making it a very attractive test [21]. Rind penetration tests have been shown to be highly correlated with lodging resistance in maize in certain studies [29,30]. Other studies showed that rind penetration tests are poorly correlated with lodging resistance [31-34]. It has been suggested that the rind puncture test can determine which maize varieties are weak to lodging forces but is less able to distinguish between varieties of moderate to high lodging resistance [35]. This thesis details a novel application of the rind penetration test to improve its effectiveness at identifying high lodging resistance maize stems.

1.4 Description of the study

The study presented in the following chapters was performed in hopes of developing a novel method of predicting stalk lodging resistance in maize. It was hypothesized that lodging resistance may be determined by performing a novel rind puncture test that traverses the entirety of the minor internode diameter of a maize stem and records the load-displacement curve. Geometric and material characteristics of the plant could be extrapolated and its lodging resistance (i.e. typically approximated as bending strength) could be estimated using a novel section modulus analogue called the Integrated Puncture Score (IPS).

The first step of the study, presented in chapter 2, was to verify that the novel rind puncture method is able to accurately determine the geometry of internodes it is used to examine. The second step of the study, presented in chapter 3, was to perform three point bending tests on a set of 1000 stalks, use the novel rind puncture method on the failed internode to calculate the IPS, and examine the correlation of failure bending stress to the IPS for each failure location. Conclusions regarding the ability of the IPS to predict stalk strength are presented in the final section of chapter 3.

This study only presents findings on stalk lodging resistance for late season (post maturation) stalk lodging in dent corn varieties. Neither green snap (stalk lodging before the plant flowering stage) nor root lodging was investigated.

Works Cited

1. Production and Exports [Internet]. U.S. Grains Council; 2020 [Cited 2020Apr21]. Available from: https://grains.org/buying-selling/corn/
2. Feedgrains Sector at a Glance [Internet]. United States Department of Agriculture Economic Research Service. United States Department of Agriculture; 2020 [cited 2020Apr21]. Available from: https://www.ers.usda.gov/topics/crops/corn-and-other-feedgrains/feedgrains-sector-at-a-glance
3. Flint-Garcia, S.A., C. Jampatong, L.L. Darrah, and M.D. McMullen. 2003. Quantitative trait locus analysis of stalk strength in four maize populations. Crop Sci. 43:13–22. doi:10.2135/cropsci2003.0013
4. Hagenbaugh, B. 2007. Corn has deep economic roots as high prices create ripple effect. USA Today 24 Jan. 2007. http://usatoday30.usatoday.com/money/industries/food/2007-01-24-corn_x.htm (verified 21 Apr. 2020).
5. Shah DU, Reynolds TPS, Ramage MH. 2017. The strength of plants: theory and experimental methods to measure the mechanical properties of stems. J Exp Bot. 2017;68:4497–516.
6. Davison B, Parks J, Davis M, Donohoe B. 2013. Plant cell walls: basics of structure, chemistry, accessibility and influence on conversion. In: Wyman CE, editor. Aqueous pretreatment of plant biomass for biological and chemical conversion to fuels and chemicals. Chichester: Wiley; 2013. p. 23–38.
7. Gibson LJ. The hierarchical structure and mechanics of plant materials. Journal of the royal society interface. 2012 Nov 7;9(76):2749-66.
8. Speck T, Burgert I. Plant stems: functional design and mechanics. Annual review of materials research. 2011 Aug 4;41:169-93.
9. Niklas, K.J. 1992. Plant biomechanics: An engineering approach to plant form and function. University of Chicago Press, Chicago.
10. Niklas, K.J. 1998. Modes of mechanical failure of hollow, septate stems. Ann. Bot. (Oxford, UK) 81:11–21. doi:10.1006/anbo.1997.0505
11. Lu, R.F., J.A. Bartsch, and A. Ruina. 1987. Structural stability of the corn stalk. ASAE. Paper No. 87-6066:1–16.
12. Kim, A.K., S.S. Cheon, M.A. Hasan, and S.S. Cho. 2004. Bending behavior of thin-walled cylindrical tube filled with aluminum alloy foam. Key Eng. Mater. 270:46–51. doi:10.4028/www.scientific.net/KEM.270-273.46

13. Chen, W.T., T. Wierzbicki, and S. Santosa. 2002. Bending collapse of thin-walled beams with ultralight filler: Numerical simulation and weight optimization. Acta Mech. 153:183–206. doi:10.1007/BF01177451
14. Schulgasser K, Witztum A. On the strength, stiffness and stability of tubular plant stems and leaves. J Theor Biol. 1992;155:497-515.
15. Schulgasser K, Witztum A. On the strength of herbaceous vascular plant stems. Ann Bot. 1997;80:35-44.
16. Crook MJ, Ennos AR. Stem and root characteristics associated with lodging resistance in four winter wheat cultivars. J Agric Sci. 1994;123:167-74.
17. Robertson DJ, Smith SL, Cook DD. On measuring the bending strength of septate grass stems. American journal of botany. 2015 Jan;102(1):5-11.
18. Robertson DJ, Julias M, Gardunia BW, Barten T, Cook DD. Corn stalk lodging: a forensic engineering approach provides insights into failure patterns and mechanisms. Crop Science. 2015;55(6):2833-41.
19. Forell GV, Robertson D, Lee SY, Cook DD. Preventing lodging in bioenergy crops: a biomechanical analysis of maize stalks suggests a new approach. Journal of experimental botany. 2015 Jul 1;66(14):4367-71.
20. Hu, H., Y. Meng, H. Wang, H. Liu, and S. Chen. 2012. Identifying quantitative trait loci and determining closely related stalk traits for rind penetrometer resistance in a high-oil maize population. Theor. Appl. Genet. 124:1439–1447. doi:10.1007/s00122-012-1799-5
21. Twumasi-Afriyie S, Hunter RB. Evaluation of quantitative methods for determining stalk quality in short-season corn genotypes. Canadian Journal of Plant Science. 1982 Jan 1;62(1):55-60.
22. Hu, H., W. Liu, L. Homann, F. Technow, H. Wang, C. Song, S. Li, A.E. Melchinger, and S. Chen. 2013. QTL mapping of stalk bending strength in a recombinant inbred line maize population. Theor. Appl. Genet. 126:2257–2266. doi:10.1007/s00122-013-2132-7
23. Lian, L., A. Jacobson, S. Zhong, and R. Bernardo. 2014. Genomewide prediction accuracy within 969 maize biparental population. Crop Sci. 54:1514–1522. doi:10.2135/cropsci2013.12.0856
24. Kokubo A, Sakurai N, Kuraishi S, Takeda K. Culm brittleness of barley (Hordeum vulgare L.) mutants is caused by smaller number of cellulose molecules in cell wall. Plant physiology. 1991 Oct 1;97(2):509-14.
25. Niklas KJ. Influence of tissue density-specific mechanical properties on the scaling of plant height. Annals of botany. 1993 Aug 1;72(2):173-9.

26. Qingting L, Yinggang O, Naxin Y. Bending load induced failure forms of sugarcane stalks. Transactions of the Chinese Society of Agricultural Engineering. 2004;20(3):6-9.
27. Berry PM, Sylvester-Bradley R, Berry S. Ideotype design for lodging-resistant wheat. Euphytica. 2007 Mar 1;154(1-2):165-79.
28. Tongdi Q, Yaoming L, Jin C. Experimental study on flexural mechanical properties of corn stalks. In2011 International Conference on New Technology of Agricultural 2011 May 27 (pp. 130-134). IEEE.
29. Anderson B, White DG, Lindell KA, Saeed AM, McCabe GP. 2430801. Evaluation of methods for identification of corn genotypes with stalk rot and lodging resistance. Plant disease. 1994;78(6):590-3.
30. Dudley JW. Selection for rind puncture resistance in two maize populations. Crop science. 1994;34(6):1458-60.
31. Butrón A, Malvar RA, Revilla P, Soengas P, Ordás A, Geiger HH. Rind puncture resistance in maize: inheritance and relationship with resistance to pink stem borer attack. Plant breeding. 2002 Oct;121(5):378-82.
32. Gou L, Huang J, Sun R, Ding Z, Dong Z, Zhao M. Variation characteristic of stalk penetration strength of maize with different density-tolerance varieties. Transactions of the Chinese Society of Agricultural Engineering. 2010 Nov 1;26(11):156-62.
33. Hu H, Meng Y, Wang H, Liu H, Chen S. Identifying quantitative trait loci and determining closely related stalk traits for rind penetrometer resistance in a high-oil maize population. Theoretical and applied genetics. 2012 May 1;124(8):1439-47.
34. Robertson DJ, Julias M, Lee SY, Cook DD. Maize stalk lodging: morphological determinants of stalk strength. Crop Science. 2017;57(2):926-34.
35. Pedersen, J., and J. Toy. 1999. Measurement of sorghum stalk strength using the Missouri-modified electronic rind penetrometer. Maydica 44:155–158.Chapter 2 – Validation of Novel Rind Penetration Technique

Chapter 2 – Measurements of Stem Morphology

2.1 Introduction

This chapter was published as a journal paper in "Plant Methods" [1] with the thesis author as primary author. It presents the findings of an exploratory study to confirm that a novel application of the rind puncture test is capable of correctly determining the diameter and rind thickness of a maize internode along the minor axis.

While this thesis focuses on lodging in maize, poison hemlock was used in this particular experiment. Poison hemlock was selected for this experiment because it is an excellent proxy for maize in regard to stem geometry (i.e. for both plants, stem diameter, rind thickness, and internode scale are very similar). Maize was not used in this particular experiment because there was limited availability of maize stems at the time.

2.2 Background

Measurements of stalk or stem diameter and rind thickness are important to physiological, biomechanical and ecological plant studies [2-7]. However, these measurements are often labor intensive, low throughput, and/or require expensive imaging equipment [8]. Measurements of rind thickness in particular typically require either expensive biomedical imaging procedures (e.g., x-Ray computed tomography) or destructive sectioning procedures that result in plant fatality (i.e. using manual or powered cutting tools) [5,9,10]. As an alternative to these procedures, the authors investigated a novel, minimally invasive rind puncture test methodology to measure rind thickness and diameter that does not induce plant fatality. The authors hypothesized that the new procedure would enable high throughput rates while maintaining measurement accuracy.

Commonly used tools to measure rind thickness and diameter in previous studies include calipers [11-13], photographic image analysis [14] and X-ray computed tomography [15]. Several methods for indirectly predicting rind thickness have also been presented. For example, correlations have been established in sorghum (sorghum bicolor) relating weight and circumference to rind thickness, thereby enabling an indirect estimation of rind thickness based on measurements of weight and circumference [16]. However, caliper measurements, image analysis, and the weight/circumference methods all require destructive and labor intensive sectioning processes that induce plant fatality. X-ray computed tomography is capable of generating accurate measurements without inducing permanent damage to the plant but has the disadvantage of being impractical for field based measurements. In addition, computed tomography requires acquisition of expensive imaging equipment / software and is fairly time intensive.

To evaluate the utility of a novel rind puncture test methodology to measure rind thickness and diameter of plant stems several measurement techniques were directly compared and contrasted. In particular, measurements of rind thickness and diameter were acquired using calipers, photographic image analysis, and the novel rind puncture test methodology. The time to complete each measurement technique along with its associated cost and accuracy were directly compared to the novel rind penetration methodology.

2.3 Methods

Description of plant materials studied

Poison hemlock samples were harvested on the morning of June 22, 2018 in Whitman County, Washington. Plants were at flowering stage, without any visible signs of disease. Each stalk was cut through the first above ground internode and through the first internode exhibiting a diameter less than 7 mm (i.e., all internode samples included in the study had a diameter larger than 7 mm). A total of 25 plants were harvested, resulting in 113 internodes total included in the study. Prior to taking any measurements each internode sample was marked with a permanent marker to indicate the locations (apical to basal) at which diameter and rind thickness measurements would be taken. All measurements and sample preparations (presented below) were accomplished within 24 hours of harvesting. All measurements of stalk diameter presented in this work refer to measurements of the stalk's minor diameter (i.e., the minimum diameter of the stalk cross-section).

Each of the 113 internodes described above was measured using three techniques (calipers, image analysis, and the novel rind puncture technique). The techniques are presented below in the same chronological order in which the experiments were conducted.

Caliper measurements of diameter

Diameter measurements were acquired using a pair of digital calipers. Diameter measurements were acquired by placing the jaws of the calipers around the stalk and repeatedly rotating the stalk to identify and mark the orientation of the minimum reading (i.e., minor diameter of the cross-section). All results were recorded on an electronic spreadsheet. Two technicians measured each internode using the same set of calipers.

Novel puncture technique – tools and setup

A Universal Testing System (Instron, model # 5944, Norwood MA) was used to puncture the center of each internode sample in the direction of the minor cross-sectional axis (i.e., in the direction of the minor diameter of the stalk) with a stainless-steel probe. The probe was 2 mm in diameter with a 45-degree 1 mm chamfer on its end (see Figure 2.1). The probe was displaced at a constant rate of 25.4 mm/sec until it had completely punctured the stalk and reached a point 5 millimeters below the zero plane. The zero plane was defined as the bottom most surface of the stalk being punctured. Figure 2.2 illustrates the test setup. Data acquisition was accomplished using Bluehill Universal testing software (Illinois ToolWorks Inc., Glenview IL). Both displacement and force were measured synchronously at a rate of 1000 samples per second.

The stalk was supported during testing, as shown in Figure 2.2, by a block support. The block support had a small void to accommodate the probe. This prevented the tested internode from being displaced vertically, and also prevented it from experiencing bending loads as the puncture test was carried out. A schematic of the upper surface of the support is shown in Figure 2.3.

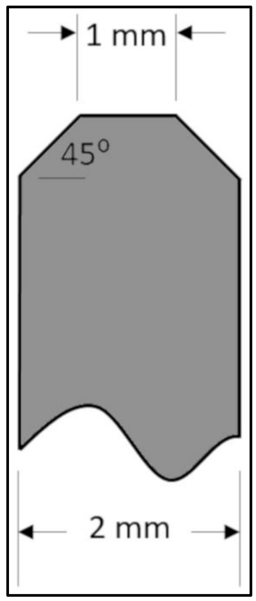

Figure 2.1: Probe tip profile

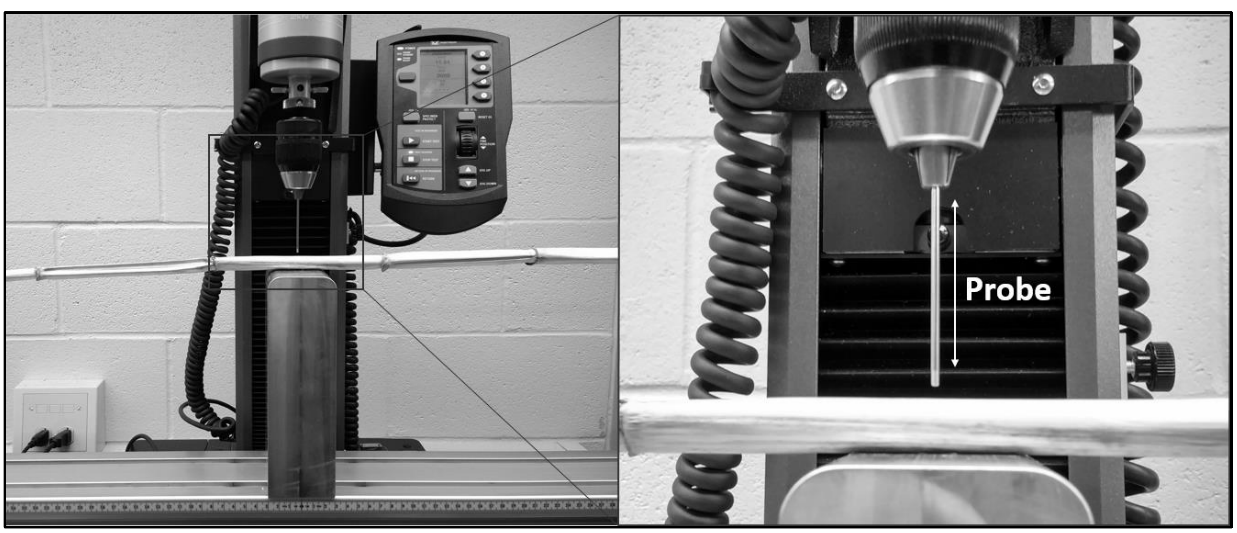

Figure 2.2: Test setup with probe, stem, and support is shown.

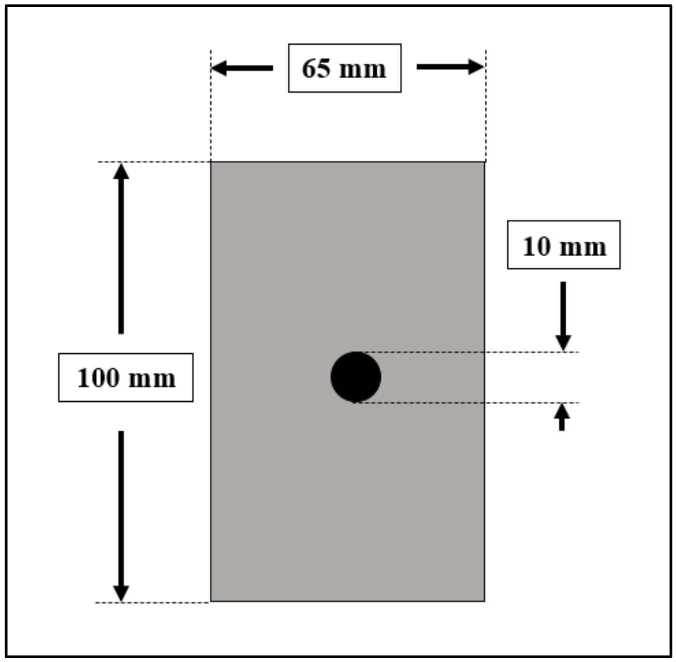

Figure 2.3: The geometry and dimensions of the support block are shown.

Novel puncture technique – test outputs

A typical force displacement graph from a rind puncture test of a poison hemlock sample in shown in Figure 2.4. A cross section of the same sample is shown above the force-displacement curve to illustrate the relationship between diameter, rind thickness and features of the force displacement graph. A custom automated MATLAB (Mathworks, Natick MA) algorithm (explained in further detail below) was developed to identify key points of the force-displacement curve generated during puncture testing and to calculate diameter and rind thickness.

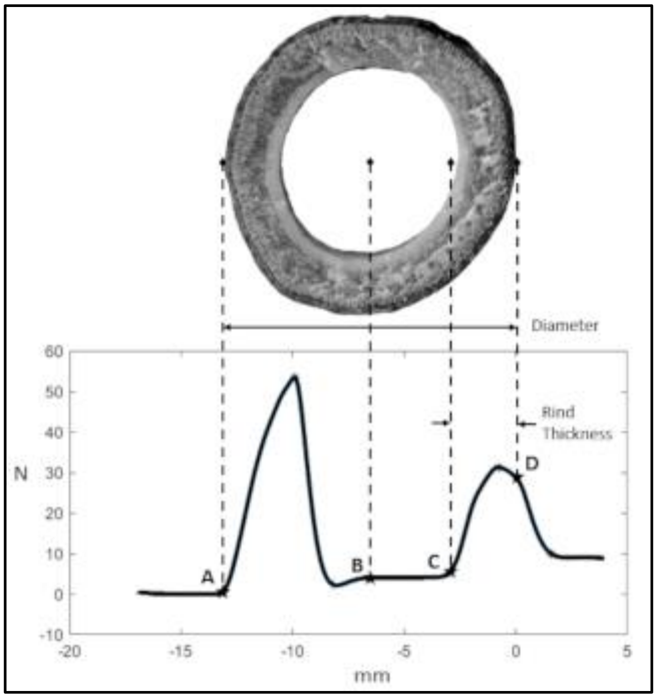

Figure 2.4:Typical load-displacement curve a puncture test of a poison hemlock sample. Maize samples produce nearly identical curves.

Novel puncture technique – algorithmic determination of morphology

The diameter was calculated by finding the distance from the point of initial contact (point A in Figure 2.4) to the zero plane (point D in Figure 2.4). The algorithm identified the point of initial contact using thresholding techniques to identify the first instance at which the force became nonzero. The first several data points were excluded from this analysis as non-zero forces occur when the probe is first put into motion due to inertial effects. After identifying the point of initial contact and the zero plane, the midpoint of the data was calculated (i.e., the center of the cross-section or point B in Figure 2.4). The rind thickness of the stalk was determined by analyzing the data between the midpoint and the zero plane. In particular, the reengagement point (point C in Figure 2.4) was identified using thresholding techniques on the second derivative of the force data to determine the point at which the force began to rapidly increase. This rapid increase in force was due to the tip of the probe reencountering the rind after traveling through the hollow center of the stalks cross-section. The rind thickness was defined as the distance between the reengagement point and the zero plane.

Caliper measurements of rind thickness

After rind puncture testing, each internode was cut in half immediately apical of the puncture location using a sharp straight edged knife. Calipers were then used to measure the rind thickness. Rind thickness measurements were acquired as near to the puncture location as possible (less than 25 mm from puncture location for all samples). Two researchers took independent measurements of rind thickness using the same set of digital calipers.

Image analysis – section acquisition

Each internode sample was then imaged and analyzed in ImageJ to determine the rind thickness and diameter. A small cross-sectional sample of the stalk was removed and scanned on an open bed scanner. If the sample broke apart or cracked while it was being sectioned, another attempt was made to cut an adjacent section. However, if the cross-sectional sample could not be made within 25 millimeters of the previous puncture and caliper measurements then no image data was collected on that internode.

Image analysis – determination of morphology

Each cross-sectional sample was placed precisely on the open bed scanner to simplify identification of the location of previous caliper measurements of rind thickness and diameter. Scans were then acquired at 2400 dots per inch in full color. Images were imported into ImageJ to determine rind thickness and diameter. In particular, the ImageJ software was used to determine diameter and rind thickness by manually selecting points in the scanned image. The distance between the points was computed in units of pixels which were then converted to lengths in millimeters using a conversion factor based on the known pixel density of the scanner settings.

2.4 Results

Sample size and essential statistics

A total of 113 poison hemlock specimens were included in the study. However, 17 fractured while trying to extract cross-sectional samples for image analysis. Image analysis results are therefore presented for 96 samples, whereas results for the puncture and caliper measurements include all 113 samples. Summary statistics including the mean, range, standard deviation and variance for measurements of diameter and rind thickness are presented in Table 2.1.

	Diameter Measurements (mm)			Rind Thickness Measurements (mm)		
	Caliper	Image Analysis	Puncture Method	Caliper	Image Analysis	Puncture Method
Mean	13.78	13.89	14.05	2.37	2.39	2.61
Range	16.84	15.96	16.42	2.76	2.76	2.97
Standard Deviation	3.17	3.096	3.71	0.6	0.62	0.71
Variance	10.03	9.59	13.75	0.35	0.39	0.51

Table 2.1: Summary of statistical features of each measurement data set.

Interuser variability

Two researchers measured each plant sample using the same set of digital calipers. The same two researchers also performed image analysis on each sample. The interuser variabilities between researchers for the diameter measurements with calipers and image analysis were 1.50% and 1.64% respectively. For the rind thickness measurements with the same tools, the interuser variabilities were 7.71% and 8.68% respectively. As the rind puncture tests were machine actuated no interuser variability data was available for the puncture test method.

Time required to measure samples

Calipers	
Measure diameter	150 min
Cut internode	150 min
Measure rind thickness	120 min
Record measurements	10 min
Total	430 min
Image Analysis	
Cut cross sections	450 min
Scan cross sections	30 min
Load images into program	20 min
Calculate rind thickness and diameter	120 min
Record measurements	10 min
Total	630 min
Rind Puncture Method	
Puncture stalks	60 min
Data analysis to calculate rind thickness and diameter	5 min
Total	65 min

Table 2.2:Comparison of time required to take measurements of diameter and rind thickness with each method. The time reported is the time to complete the measurements for all 113 samples in the study.

The time required to perform each measurement was recorded to enable comparison of each methods potential for high throughput phenotyping. Table 2.2 shows a comparison of the time required to prepare samples for measurement and the time required to carry out each step of the measurement.

Agreement between methods

Linear correlation analysis was employed to compare the results of the three measurement techniques employed in this study (i.e., image analysis, caliper measurements and the novel rind puncture technique). Table 2.3 shows the coefficients of correlation between each method. The average diameter and rind thickness values from the two researchers who took image analysis and caliper measurements were used to compute the coefficients of correlation presented Table 2.3. All methods showed strong agreement, indicating the ability of the rind puncture method to obtain accurate measurements of rind thickness and diameter.

R^2 values between methods – Diameter		
	Caliper	Image Analysis
Puncture Method	0.9939	0.9700
R^2 values between methods – Rind Thickness		
`	Caliper	Image Analysis
Puncture Method	0.8623	0.8410

Table 2.3: Comparison of R2 values between each measurement method.

2.5 Discussion

Cost of tools

Each measurement method used in this study required at least one tool. The caliper method required a pair of digital calipers. A representative cost of a pair of digital calipers is $20 to $100. The image analysis technique required a computer, a scanner, and software. The cost of the computer and scanner together are estimated at $400 to $1,000. The software (i.e. ImageJ) was open source and therefore incurred no cost. The rind puncture method required an Instron universal testing frame, a computer, and a MATLAB license. Together, these items cost approximately $50,000. In summary, the most expensive method was the rind puncture method by a wide margin, while the least expensive was the caliper method.

Training required

Training for all three methods took approximately the same amount to time to carry out. For the caliper method, a 10-minute demonstration of proper caliper usage was all that was required. For the image analysis method, researchers watched a 10-minute video to familiarize themselves with the software tools they would be using. For the rind puncture method, training consisted of a 10-minute demonstration of the procedure. In other words, each method required approximately 10 minutes of training.

Time to complete measurements

The total time spent by all researchers in carrying out the various measurements are summarized in Table 2.2. The image analysis method was the most time consuming, requiring 630 minutes to complete. The most time intensive process for image analysis was sectioning the stalk samples (450 minutes). The caliper method was the next most time intensive requiring 430 minutes to complete. The least time intensive method was the rind puncture method, which required only 65 minutes. It should be noted that several automated image analysis algorithms have been presented in the literature that could reduce the time to scan and compute stalk diameter and rind thickness [6,7,17-22]. However, the authors are unaware of any reported high throughput sectioning procedures that would reduce time to section stalk cross-sections below the reported 450 minutes required in this study. Thus, the rind puncture methods would still be significantly faster even if automated image analysis algorithms were employed.

Interuser variability

Inter user variability was measured for the caliper and image analysis methods and was found to be small to moderate (< 2% for diameter measurements and < 9% for rind thickness measurements). Because a given measurement site can only be punctured a single time, no comparisons of inter user variability were made for the puncture method. The authors expect inter user variability for rind thickness measurements to be significantly higher when measuring pith filled plant stems as it can be difficult to determine the boundary between pith and rind.

Agreement between methods

To determine the level of agreement between measurement systems a linear correlation analysis was conducted. Each system exhibited coefficients of determination (R^2 values) greater than 0.84 (see Table 2.3). The high level of agreement between the different methods suggests that any of these methods could be used to obtain accurate measurements of rind thickness and diameter. The attendant advantages and disadvantages of each method are discussed in the sections below.

Advantages/disadvantages of caliper measurements

Calipers are an inexpensive tool. They are easy to obtain and easy to use. They can be used with equal ease in a laboratory or in the field. However, their capacity for high throughput measurements of rind thickness is limited, making measurements of large sample sets impractical. Calipers would be a preferred tool in studies requiring immediate measurements of rind thickness of plant stalks/stems for a relatively small sample set (i.e., < 100 samples/user).

Advantages/disadvantages of image analysis measurements

The Image analysis method to determine stalk/stem diameter and rind thickness was effective but required more sample preparation (i.e. cutting a thin cross section capable of being placed on a flatbed scanner) than the other two methods. In this study 15% of the samples (i.e. 17 internodes) were destroyed during sectioning. This method requires tools that are not easily portable to the field, limiting this method primarily to laboratory settings. Image analysis would be a preferred method for experiments requiring measurements of rind thickness of small to large sample sizes in laboratory settings, so long as the samples are easy to section. An added advantage of the image analysis method is that it does not requiring contacting the sample. When measuring soft or deformable samples caliper readings are highly dependent upon the amount of force the user applies to the sample. Image analysis techniques and other non-contact methods are often more suited to measure such samples as compared to calipers.

Another advantage that image analysis techniques exhibit is the permanent, verifiable record of sample geometry. Where the other methods examined in this study rely on records of the measurements taken, imaging techniques allow for remeasurements and the application of new measures to the same sample set. In certain studies, it may be worth the extra time and effort required to section and image samples to have such a permanent record of the samples.

Advantages/disadvantages of the rind puncture method

The rind puncture method is the only non-lethal method of measuring rind thickness that could potentially be used in a field setting. For example, puncture tests are frequently used in field studies of maize (*Zea mays*) and other grasses to assess stalk strength without inducing plant fatality[19]. In this study a universal material testing frame / system was used to conduct the puncture tests. Materials testing frames are largely immobile and inappropriate for field work. The authors chose to use a universal testing frame to validate the puncture test methodology. However, they are currently developing a portable handheld device to conduct puncture tests of plant stems and stalks. The primary advantage of such a device would be the ability to determine stalk diameter and rind thickness in the field without inducing plant fatality. The authors are not aware of any other methods to non-destructively measure rind thickness in a field. In the meantime, laboratory-based puncture tests which utilize a universal testing system can offer a high degree of automation, allowing for high throughput measurements of rind thickness and diameter. Such tests are best suited for large sample sets (> 100 samples). Table 2.4 presents a quantitative summary of each methods advantages and disadvantages. The last column of the table presents the average of the R2 values between the given technique and the two other methods investigated in the study.

	Equipment cost	Training Time	Time to measure 113 samples	Inter user Variability	Average R^2 (Diameter)	Average R^2 (Rind Thickness)
Caliper	~ $50	10 min	430 min	1.5% & 7.71%	0.9854	0.8854
Image Analysis	~ $500	10 min	630 min	1.64 & 8.68%	0.9735	0.8748
Puncture Method	~ $50,000	10 min	65 min	Not studied, Assumed negligible	0.9820	0.8517

Table 2.4: Summary of advantages and disadvantages of each measurement system

Complexity of obtaining accurate rind thickness measurements

Rind thickness measurements for all methods demonstrated lower R^2 values than diameter measurements. This was partly due to difficulty associated with identifying the correct plane of measurement. For example, for the image analysis and caliper measurements there was uncertainty as to what two points should be used to calculate rind thickness when a geometric irregularity in the stalk cross-section was at or near the measurement location. Caliper measurements of rind thickness were also sensitive to variations in pressure applied by the user.

2.6 Conclusions

The rind puncture technique described here is a viable method to obtain measurements of rind thickness and diameter. The method is non-lethal, easy to perform, and has high throughput. It is recommended for use in studies with large sample sets. The authors are currently working to develop a custom handheld apparatus to allow the novel rind puncture method to be used in field work.

Works Cited

1. Seegmiller WH, Graves J, Robertson DJ. A novel rind puncture technique to measure rind thickness and diameter in plant stalks. Plant methods. 2020 Dec;16(1):1-8.
2. Prest TJ, Cantrell RP, Axtell JD. Heritability of lodging resistance and its association with other agronomic traits in a diverse Sorghum population 1. Crop Sci. 1983;23(2):217–21.
3. Arnold JM, Josephson LM. Inheritance of stalk quality characteristics in maize 1. Crop Sci. 1975;15(3):338–40.
4. Esechie HA, Rodriguez V, Al-Asmi H. Comparison of local and exotic maize varieties for stalk lodging components in a desert climate. Eur J Agron. 2004;21(1):21–30.
5. Esechie H. Relationship of stalk morphology and chemical composition to lodging resistance in maize (Zea mays L.) in a rainforest zone. J Agric Sci. 1985;104:429–33.
6. Davis SM, Crane PL. Recurrent selection for rind thickness in maize and its relationship with yield, lodging, and other plant characteristics 1. Crop Sci. 1976;16(1):53–5.
7. Robertson DJ, Julias M, Lee SY, Cook DD. Maize stalk lodging: morphological determinants of stalk strength. Crop Sci. 2017;57(2):926–34.
8. Gomez FE, Carvalho G, Shi F, et al. High throughput phenotyping of morpho-anatomical stem properties using X-ray computed tomography in sorghum. Plant Methods. 2018;14:59. https ://doi.org/10.1186/s1300 7-018-0326-3.
9. Heckwolf S, Heckwolf M, Kaeppler SM, et al. Image analysis of anatomical traits in stalk transections of maize and other grasses. Plant Methods. 2015;11:26. https ://doi.org/10.1186/s1300 7-015-0070-x.
10. Al-Zube LA, Robertson DJ, Edwards JN, et al. Measuring the compressive modulus of elasticity of pith-filled plant stems. Plant Methods. 2017;13:99. https ://doi.org/10.1186/s1300 7-017-0250-y.
11. Zuber MS, Grogan CO. A new technique for measuring stalk strength in corn. Crop Sci. 1961;1:378–80.
12. Zhang Y, Legay S, Barrière Y, Méchin V, Legland D. Color quantification of stained maize stem section describes lignin spatial distribution within the whole stem. J Sci Food Agric. 2013;61:3186–92.
13. Legland D, Devaux MF, Guillon F. Statistical mapping of maize bundle intensity at the stem scale using spatial normalization of replicated images. PLoS ONE. 2014;9:e90673.

14. Shamir L, Orlov N, Eckley DM, Macura T, Johnston J, Goldberg IG. Wnd-chrm—an open source utility for biological image analysis. Source Code Biol Med. 2008;3(1):13.
15. Pau G, Fuchs F, Sklyar O, Boutros M, Huber W. EBImage—an R package for image processing with applications to cellular phenotypes. Bioinformat-ics. 2010;26(7):979–81.
16. Dao D, Fraser AN, Hung J, Ljosa V, Singh S, Carpenter AE. Cell Profiler Analyst: interactive data exploration, analysis and classification of large biological image sets. Bioinformatics. 2016;32(20):3210–2.
17. Rajaram S, Pavie B, Wu LF, Altschuler SJ. PhenoRipper: software for rapidly profiling microscopy images. Nat Methods. 2012;9(7):635–7.
18. Schindelin J, Arganda-Carreras I, Frise E, Kaynig V, Longair M, Pietzsch T, Preibisch S, Rueden C, Saalfeld S, Schmid B, Tinevez JY, White DJ, Harten-stein V, Eliceiri K, Tomancak P, Cardona A. Fiji: an open-source platform for biological-image analysis. Nat Methods. 2012;9(7):676–82.
19. Twumasi-Afriyie S, Hunter RB. Evaluation of quantitative methods for determining stalk quality in short-season corn genotypes. Can J Plant Sci. 1982;62(1):55–60.
20. Thompson TL. Temporary storage of high-moisture shelled corn using continuous aeration. Trans ASAE. 1972;15(2):333–0337.
21. Heckwolf S, Heckwolf M, Kaeppler SM, de Leon N, Spalding EP. Image analysis of anatomical traits in stalk transections of maize and other grasses. Plant Methods. 2015;11(1):26.
22. McAuley R. Effects of potassium on stress-induced stalk lodging of grain sorghum (Sorghum bicolor) (Doctoral dissertation). Kansas State University; 1973.
23. Zhang Y, Zhao C, Du J, Guo X, Wen W, Gu S, Wang J, Fan J. Crop phenomics: current status and perspectives. Front Plant Sci. 2019;10:714.
24. Duvick DN. The contribution of breeding to yield advances in maize (Zea mays L.). Adv Agron. 2005;86:83–145.
25. Stubbs CJ, Seegmiller K, Sekhon RS, Robertson DJ. Are maize stalks efficiently tapered to withstand wind induced bending stresses? bioRxiv. 2020. https ://doi.org/10.1101/2020.01.21.914804.

Chapter 3 – Generating a Predictive Score

3.1 Introduction

Purpose of the chapter

This chapter presents the method of calculating a quantity called the Integrated Puncture Score (IPS) using puncture data obtained from the puncture method described in chapter 2. The algorithm used to calculate the IPS is presented. The effectiveness of the IPS for predicting lodging resistance is determined experimentally and validated with statistical methods. The remaining sections of this chapter have been submitted and are currently under review for publication as a peer reviewed journal paper. A non-peer reviewed preprint of the article can be found at [1] with the thesis author as contributing author.

3.2 Background

Stalk lodging (permanent displacement of plants from their vertical orientation) severely reduces agronomic yields of several vital crop species including maize. Yield losses due to stalk lodging are estimated to range from 5-20% annually [2,3]. Stalk lodging, as opposed to root lodging, occurs when the mechanical stability of the plant is lost due to structural failure of the plant stem [4,5].

To estimate stalk strength and stalk lodging resistance of large grain crops plant scientist frequently utilize rind puncture tests [6–21]. Despite nearly 100 years of research the rind puncture method remains virtually unchanged from the time at which it was first introduced to the research community. In particular, the method consists of simply measuring the peak penetration force required to insert a probe through a plant's rind. The underlying assumption is that the penetration force is related to the material properties of the rind tissue which is in turn related to stalk bending strength / lodging resistance. Numerous researchers have demonstrated that rind puncture resistance measurements correlate with stalk lodging resistance [7,9,10,21,22].

However, the rind puncture method has not been widely adopted by breeding programs and it suffers from two key limitations. First, although rind penetration measurements have been shown to correlate with stalk lodging, the predictive power of the test decreases significantly when measuring elite or pre-commercial hybrids thus limiting its utility in late stage breeding trials [21,23,24]. Second, using rind penetration measurements as a breeding metric does not necessarily create stronger stalks [7,21]. For example, repeated selection for rind penetration resistance has been shown to produce stalks with smaller diameters [7]. Stalks with smaller diameters are known to be structurally inferior to stalks with larger diameters [24]. Thus, using rind penetration resistance as a selective breeding metric can produce stalks with a structurally disadvantageous morphology. In other words, rind penetration measurements do not measure or account for cross-sectional geometries or the spatial distribution of material stiffness within the plant, both of which are known to be highly correlated with stalk lodging resistance [24,25].

The purpose of this study is to present a methodology for a modified rind penetration measurement that addresses these limitations by integrating both the tissue stiffness and the distribution of that stiffness into a single measurement called the "Integrated Puncture Score‟. It is anticipated that the new method will enable plant breeders to use rind penetration tests to (1) better assess elite hybrids for stalk lodging resistance and (2) be used directly as a selective breeding index to improve stalk lodging resistance.

3.3 Methods

Experimental materials

Two unique sets of maize hybrids were utilized in this study. The first set of hybrids were selected to represent a reasonable portion of maize genetic diversity and morphology. The second set consisted solely of elite commercial hybrids. The first set was chosen to mimic the type of diversity encountered when conducting diversity panel experiments. The second set was chosen to mimic the type of diversity encountered in late stage pre-commercial breeding trials. Hereafter the first set will be referred to as the “Diversity Set” and the second set will be referred to as the “Commercial Set”. More information about each set of hybrids and the sampling strategy for each set is given below.

The Diversity Set of maize stalks was chosen to represent a reasonable portion of maize genetic diversity and were selected for variation in stem morphology and biomass distribution. The hybrids were planted at Clemson University Simpson Research and Education Center, Pendleton, SC in well drained Cecil sandy loam soil. The hybrids were grown in a Random Complete Block Design with two replications. In each replication, each hybrid was planted in two-row plots with row length of 4.57 m and row-to-row distance of 0.76 m with a targeted planting density of 70,000 plant ha^{-1}. The experiment was surrounded by non-experimental maize hybrids on all four sides to prevent any edge effects. To supplement nutrients, 56.7 kg ha^{-1} nitrogen, 86.2 kg ha^{-1} of phosphorus and 108.9 kg ha^{-1} potassium was added at the time of soil preparation, and additional 85 kg ha^{-1} nitrogen was applied 30 days after emergence. Standard agronomic practices were followed for crop management.

The Commercial Set of maize stalks consisted of five commercial varieties of dent corn grown during the 2013 season at Monsanto facilities in Iowa in a randomized block design which included planting densities of 119000, 104000, 89000, 74000, and 59000 plants ha–1 (48000, 42000, 36000, 30000, and 24000 plants ac –1), two locations, and two replicates. Additional information about the origin and sampling of these stalks can be found in a previous report [24].

All stalks used for this study were harvested when all the hybrids were either at or past physiological maturity (i.e., 40 days after anthesis). Ten competitive plants from each replication were harvested by cutting at just above ground level, stripped of all the leaves and ears, and transferred to a forced air dryer for drying. Some plots lacked 10 competitive plants and, therefore, the total number of plants evaluated for each hybrid varied slightly. In total, 841 (Diversity Set) and 933 (Commercial Set) fully mature, dried maize stalks were used in this study. All stalks included in the study (from both the Diversity and Commercial Sets) were submitted to 3-point bending and rind penetration tests as described below.

3-point bending

Three-point bending tests were performed on all stalk specimens. A Universal Testing System (Instron Model # 5944, Norwood MA) was used to perform the tests. Stalks were loaded at nodes to avoid premature local failure because of cross sectional compression in the weaker internodal regions [3,25]. Each stalk was supported on their uppermost and lowermost (apical to basal) nodes. Specimens were loaded until failure, and the maximum bending moment was recorded. Load-displacement data was collected using Bluehill Universal Testing Software (Illinois TookWorks Inc., Glenview IL). Further detail on the method can be found in [3,26].

Rind puncture testing

Rind puncture tests were performed on all stalk specimens. In particular, a Universal Testing System (Instron, model # 5944, Norwood MA) was used to puncture the centermost internode of each stalk sample in the direction of the minor cross-sectional axis (i.e., in the direction of the minor diameter of the stalk) with a stainless-steel probe. The probe was 2mm in diameter with a 45 degree 0.5mm chamfer on its end. The probe was lowered until it had completely punctured the entirety of the stalk cross-section. Note this is slightly different than a typical rind puncture test. In a traditional rind penetration test the probe is typically retracted after reaching the center of the stalk cross-section and the maximum force is recorded. In this study synchronous load and displacement data from each penetration tests were acquired using Bluehill Universal Testing Software (Illinois TookWorks Inc., Glenview IL). Load displacement data were acquired at a rate of 1000 samples per second and the probe was actuated at a rate of 25 mm/s. Further details on the puncture method and probe geometry can be found in previous studies from our lab [5,20]. For this study the "traditional rind puncture measurement" was attained by determining the maximum load (i.e. force) that occurred in the puncture test prior to the tip of the probe passing the midpoint of the stalk cross-section. The Integrated Puncture Score was calculated as described below.

Integrated Puncture Score

The Integrated Puncture Score for each stalk was calculated using a custom Matlab algorithm. The algorithm was developed using structural engineering principles and theory that govern the flexural response of engineering structures. In particular the algorithm was designed to simultaneously account for the cross-sectional distribution and puncture strength of stalk tissues. The underlying theory and mechanics of the algorithm is described below.

A typical load-displacement curve from a rind puncture test of a maize stalk is shown in Figure 3.1a. As shown in Figure 3.1 the penetrating probe makes initial contact with the stalk specimen at (Figure 3.1a - Point A). After initial contact the load rapidly increases until the probe penetrates the rind tissue (Figure 3.1a - Point B). A rapid decrease in load is observed as the probe begins to enter the pith tissues (Figure 3.1a - Point C). The load maintains a relatively low force as the probe is driven through the specimen's pith (Figure 3.1a - Points C to E). When the probe engages with the rind tissues on the far side of the stalk cross-section the load rapidly increases again (Figure 3.1a - Point E). The tip of the probe typically passes the pre-calibrated zero deflection point (i.e., the back side of the stalk cross-section, Figure 3.1a - Point F), and continues increasing in load until it breaks through the far-side of the specimen (Figure 3.1a - Point G). Note the peak force does not necessarily coincide with the Point F. This is due to complex fracture mechanics, rapid crack propagation, and slight deflections of the rind tissue that occur during puncturing testing. The Integrated Puncture Score algorithm extracts these points using peak identification and slope thresholding algorithms as described in a previous study from our lab [21].

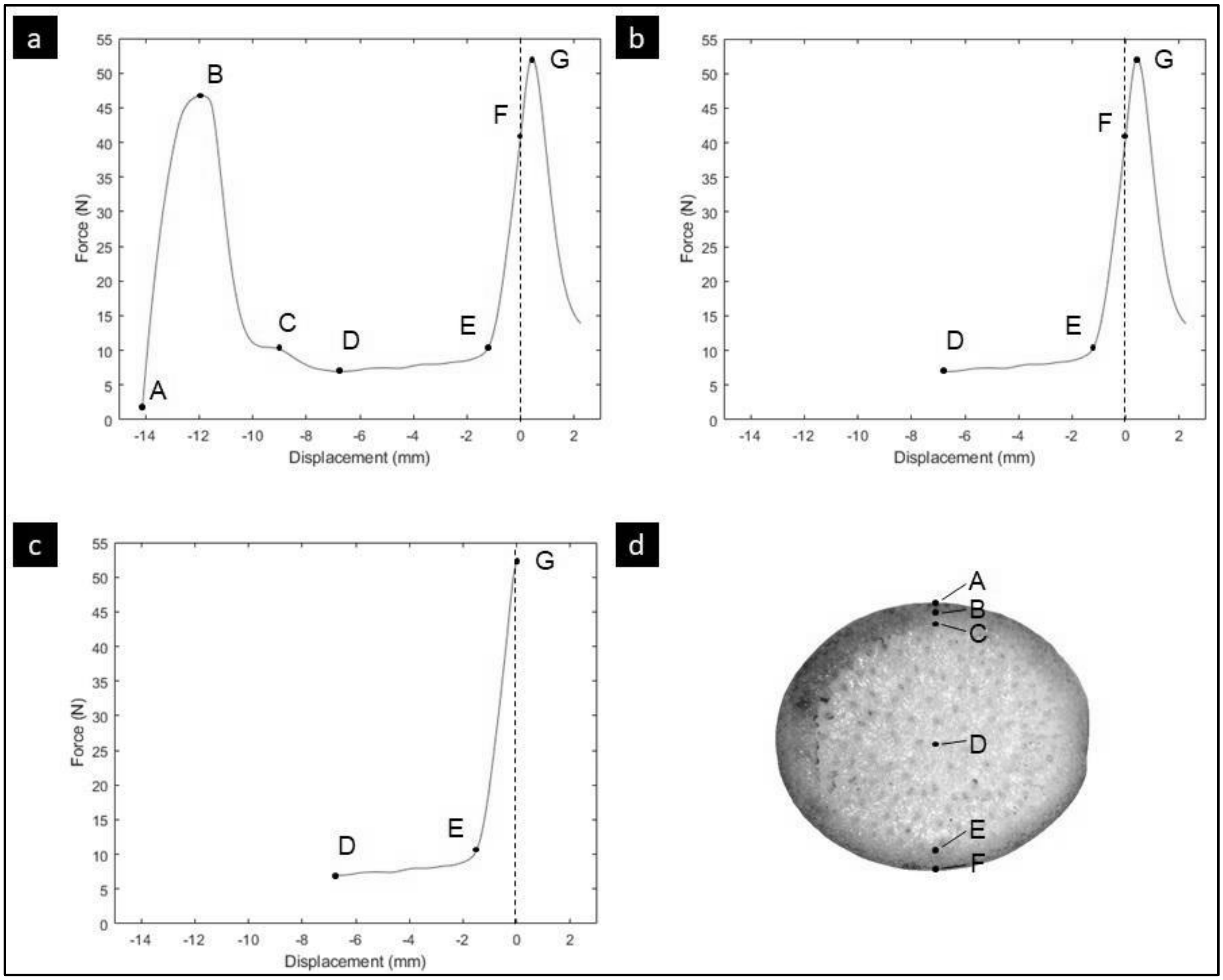

Figure 3.1: (a) A typical force-distribution curve from a rind penetration test; key points on the plot are as follows: Point A - entry point, Point b - first peak, Point C - first rind-pith transition, Point D - midpoint, Point E - second rind-pith transition, Point F – precalibrated displacement plane (i.e. the backside of the stalk), Point G – second peak. (b) The first half of the graph is removed. (c) The displacement values are scaled such that point G occurs at zero displacement. (d) A test specimen with the key points labeled.

Once these points have been identified, the Integrated Puncture Score algorithm performs several additional pre-analysis steps, as shown in Figure 3.1b and Figure 3.1c. First, the midpoint of the stalk cross-section (point D) is defined as lying halfway between Points A and F. Data from the initial contact of the probe with the stalk (Point A) to the midpoint of the stalk cross-section (Point D) is then removed. Second, the data from the midpoint (Point D) to the peak load (Point G) is scaled in the x-direction such that Point G (the peak load) will coincide with the zero-plane (Point F). Figure 3.1d displays a typical stalk cross-section with labeled points corresponding to points A-F in Figure 3.1a, 3.1b and 3.1c.

To calculate the Integrated Puncture Score, the scaled data shown if Figure 3.1c are numerically integrated to derive a material weighted section modulus analog. A typical material weighted section (S_E) modulus calculation of a heterogenous material would take the form [26]:

$$S_E = \frac{\int_A E\, x^2 dA}{x_{max}} \tag{1}$$

where E is the tissue modulus of elasticity, and x is the distance of that tissue to the neutral bending layer of the structure in question with x having a maximum value denoted as x_{max}. A similar approach is used to calculate the Integrated Puncture Score. In particular, we calculate the Integrated Puncture Score by numerically integrating the curve in Figure 3.1c and using the penetrating force as an approximate measure of tissue stiffness or strength. In other words, the penetrating force is weighted by the fourth power of the distance to the neutral layer (point D):

$$IPS = \left(\sum_{n\,=\,Point\ D}^{Point\ G} F_n \cdot {x_n}^4 - F_{n-1} \cdot {x_{n-1}}^4 \right) \Big/ x_{max} \tag{2}$$

Where the resulting value matches Equation 1 in units of *puncture force* x *length*^{3}.

Empirical model

To validate the Integrated Puncture Score as an efficient and appropriate aggregation of the observed force curve data, we analyze the same using a functional regression model. The premise, the proposed functional regression model holds the form of the Integrated Puncture Score as a special case thus if the fitted value of the functional regression model coincides with Integrated Puncture Score then this validates it as the best aggregation of the observed information. To this end, let Y_i denote the strength measurement taken on the ith stalk, for i = 1, ..., m. Further, let $F_i(x)$ denote the corresponding force curve at the xth position.

To relate strength to the force curve we posit the following functional regression model

$$Y_i = \gamma_0 + \int \beta(x) F_i(x) dx + \epsilon_i, \tag{3}$$

Where ϵ_i, for $i = 1, \dots, m$, are homoscedastic mean-zero random errors that are uncorrelated with each other, γ_0 is an intercept parameter, and $\beta(x)$ is an unknown functional coefficient; for further discussion on functional regression models see Ramsay and Silverman (2007). It is important to note that $\beta(x)$ is an infinite dimensional parameter. Thus, to reduce the dimensionality of the problem, we approximate this parameter via B-splines (see Schumaker, 2007); i.e., as

$$\beta(x) = \sum_{j=1}^{J} B_j(x) \gamma_j \tag{4}$$

where $B_j(x)$ is a B-spline basis function and γ_j is the corresponding spline coefficient, for j = 1, …, J. These basis functions are fully determined once a knot sequence and degree are specified; for further discussion see Schumaker (2007). For adequate modeling flexibility, in this application we use a knot set consisting of 7 interior knots (placed at equally spaced quantiles) and specified the degree to be 3. To smoothly estimate the functional coefficient, we use a regularizing penalty; i.e., our objective function takes on the form

$$\widehat{\boldsymbol{\gamma}}_{\lambda} = argmin_{\boldsymbol{\gamma}} \sum_{i=1}^{m} \{Y_i - \gamma_0 + \int \beta(x) F_i(x) dx\}^2 + \lambda \int \{\beta^{(1)}(x)\}^2 dx, \tag{5}$$

where $\boldsymbol{\gamma} = (\gamma_0, \gamma_1, \dots, \gamma_J)'$ is the collection of unknown parameters, λ is a penalty parameter, $\widehat{\boldsymbol{\gamma}}_{\lambda}$ is a penalty parameter specific estimator of $\boldsymbol{\gamma}$, and $\beta^{(1)}(x)$ is the first derivative of $\beta(x)$. To 212 choose the penalty parameter we first note that

$$\widehat{\boldsymbol{\gamma}}_{\lambda} = \{\boldsymbol{M}'\boldsymbol{M} + \boldsymbol{R}^{*}(\lambda)\}^{-1}\boldsymbol{M}'\boldsymbol{Y}, \tag{6}$$

where $\boldsymbol{Y} = (Y_1, \dots, Y_m)'$, $\boldsymbol{M} = (\boldsymbol{M}_1', \dots, \boldsymbol{M}_n')'$, $\boldsymbol{M}_i = (1, B_1(x)X_i(x), \dots, B_J(x)X_i(x))'$, and $\boldsymbol{R}^{*}(\lambda)$ is a $(J+1) \times (J+1)$ matrix whose first row and column are all zeros and whose remaining entries are given by $\boldsymbol{R}^{*}(\lambda)_{jj'} = \lambda B_{j-1}^{(1)}(x) B_{j'-1}^{(1)}(x)$. Thus, we chose the penalty parameter to be the value of λ that minimizes the usual Schwartz Bayesian Information Criterion (BIC) with the "degrees of freedom" being specified as $df(\lambda) = tr(\boldsymbol{S}_{\lambda})$, where $\boldsymbol{S}_{\lambda} = \boldsymbol{M}\{\boldsymbol{M}'\boldsymbol{M} + \boldsymbol{R}^{*}(\lambda)\}^{-1}\boldsymbol{M}'$

and $tr(\boldsymbol{S}_{\lambda})$ denotes the trace of the matrix $\boldsymbol{S}_{\lambda}$.

3.4 Results

To test the hypothesis that rind penetration tests predict stalk bending strength, a series of statistical analyses were performed. To formally examine this stated hypothesis, we posit and fit a linear regression model where log-rind-puncture-resistance or log-Integrated-Puncture-Score is the predictor variable and log-strength is the response variable of interest. Figure 3.2 depicts the results of these linear regressions. For the Diversity Set, we find that both Integrated Puncture Score (R^2 = 0.67) and RPR (R^2 = 0.67) are associated with bending strength. For the Commercial Set, we find that as hypothesized the association with Integrated Puncture Score remains high (R^2 = 0.74), but the association with traditional rind puncture resistance decreases (R^2 = 0.48).

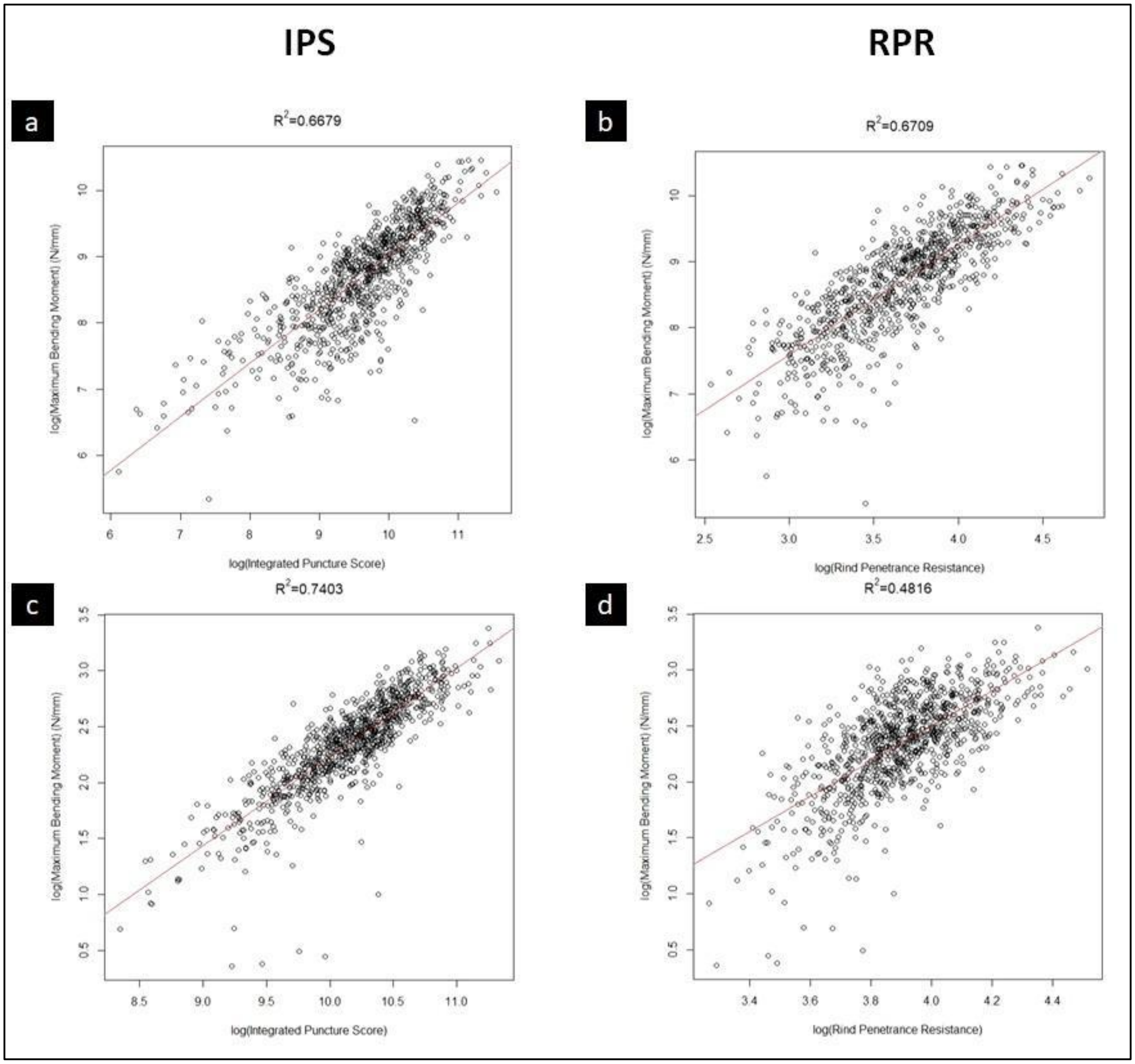

Figure 3.2: A linear regression model of log-Strength with log-Integrated Puncture Score (a, c) and log-RPR (b, d).

A further analysis was conducted to test the assertion that the Integrated Puncture Score is better able to distinguish elite hybrids for stalk lodging resistance than tradition rind puncture techniques. In particular, we reanalyzed the Diversity Set leaving out the nth weakest percentile, where n was allowed to range from 0-80 percent. In other words, the weakest stalks were systematically discarded from the analysis and the R^2 values between stalk bending strength and each puncture test technique were reevaluated. Figure 3.3 depicts the R^2 values of each technique as a function of n (percentile strength). As seen in Figure 3.3 the Integrated Puncture Score demonstrates a stronger association with stalk bending strength especially when only elite specimens (i.e., strong stalks) are included in the analysis.

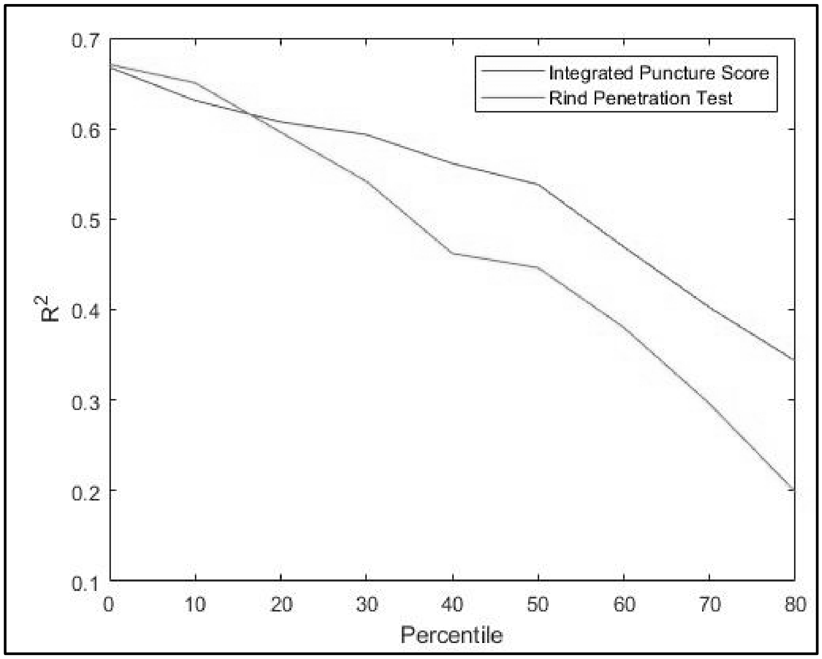

Figure 3.3: R2 values of the regression between log-RPR and log-Integrated Puncture Score with log-bending strength when removing the nth weakest percentile of stalks from the Diversity dataset (e.g. when "Percentile" is equal to 30, the linear regression is only performed on the strongest 70th percentile of stlaks). Integrated Puncture Score has stronger correlation theatn the traditional rind penetration tests and is more robust when looking at stronger, more elite plants.

Comparing other metrics to the maximum bending load

To further establish the relative effectiveness of the Integrated Puncture Score, additional metrics and their correlation to the maximum bending moment are presented in Table 3.1. Each R^2 value is presented for log-log axis scaling between the named variable and the maximum bending moment. No variable presented in Table 3.1 had its correlation significantly reduced by using log-log scaling over linear scaling.

The section modulus correlation, as shown in Table 3.1, was calculated using the formula for section modulus[37] for a circle as shown below, with the minor diameter in place of the circle diameter.

$$SM = \frac{\pi d^3}{32}$$

The load-displacement curve integral is simply the integral of the entire load-displacement curve (i.e. as shown in Figure 3.1a). The IPS-x^3, was calculated with the same summation as the Integrated Puncture Score, except that all distance weighting was accomplished by raising to the third power instead of to the fourth. The IPS outperforms the variables listed in Table 3.1 by a significant margin (i.e. by 15.7% in the nearest case).

Correlation between maximum bending moment and measured variables.	
Variable	**R^2**
Rind Thickness	0.2954
Diameter	0.3014
Section Modulus	0.3129
Load-Displacement Curve Integral	0.5729
IPS-x^3	0.6243

Table 1.1:Non IPS variables and their correlation with maximum bending moment. Presented for comparison between the IPS and related variables.

Comparison of Integrated Puncture Score to empirical model

As a point of validation [28], we examine the hypothesis that the Integrated Puncture Score is the best way to aggregate the synchronous load-displacement data captured during a puncture test to explain strength. This is evaluated by fitting the functional regression model (which holds the

Integrated Puncture Score aggregation as a special case) to the strength data. The fitted values (i.e. the estimated value of the linear predictor from the functional regression analysis) is then compared to the Integrated Puncture Score. Figure 3.4 depicts the results of Integrated Puncture Score vs. the fitted values from the empirical functional regression analysis. It is found that the fitted values from the empirical model and the Integrated Puncture Score are highly correlated for both the Diversity Set (R^2 = 0.92) and the Commercial Set (R^2 = 0.94), which suggest two findings. First, the Integrated Puncture Score captures the features of the load-displacement curve that most closely relates to the bending strength of the specimen. Second, this relationship does not seem to be sensitive to the data set used, i.e. Integrated Puncture Score accurately captures the correct features for both a wide array of hybrids as well for elite hybrids.

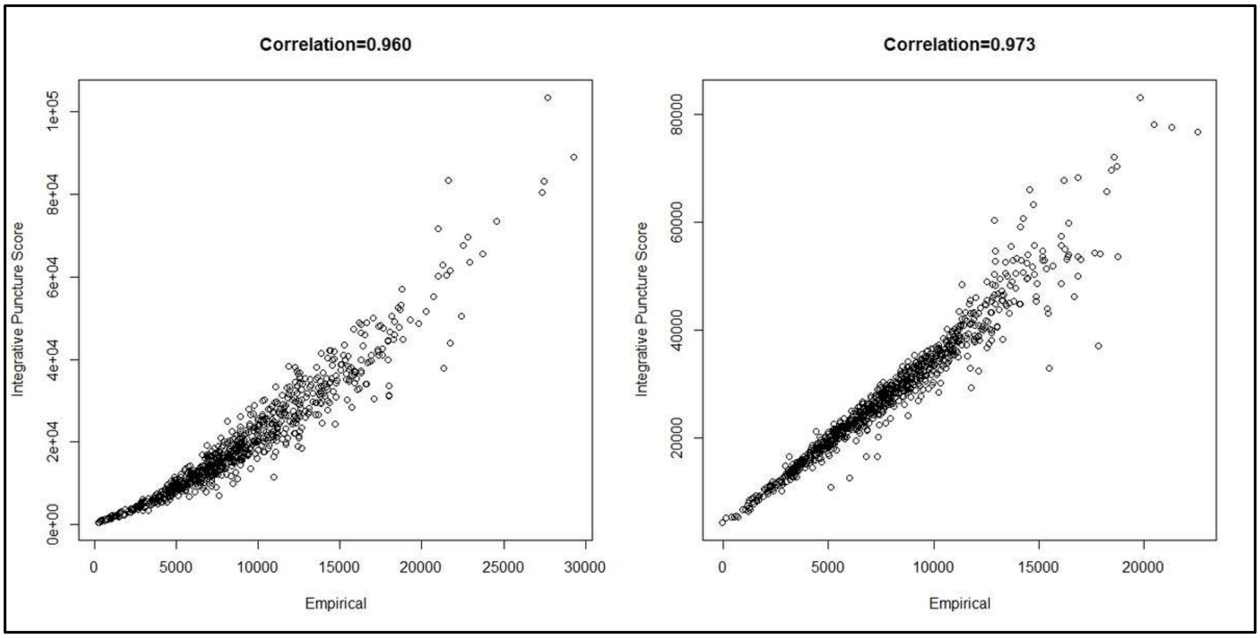

Figure 3.4: Scatter plot of the Integrated Puncture Score vs. fitted values arising from the empirical model for the Diversity Set (left) and the Commercial Set (right) of maize stalks.

Integrated Puncture Score can Differentiate the Strength of Hybrids

To test the hypothesis that Integrated Puncture Score can differentiate the bending strength of hybrids, a series of statistical analyses were performed on the data. Figures 3.5 and 3.6 provide a depiction of the variation (via boxplots) in bending strength by hybrid type. As expected, these figures indicate substantial variation in bending strength across hybrids for the Diversity Set, and minimal variation in bending strength across hybrids for the Commercial Set.

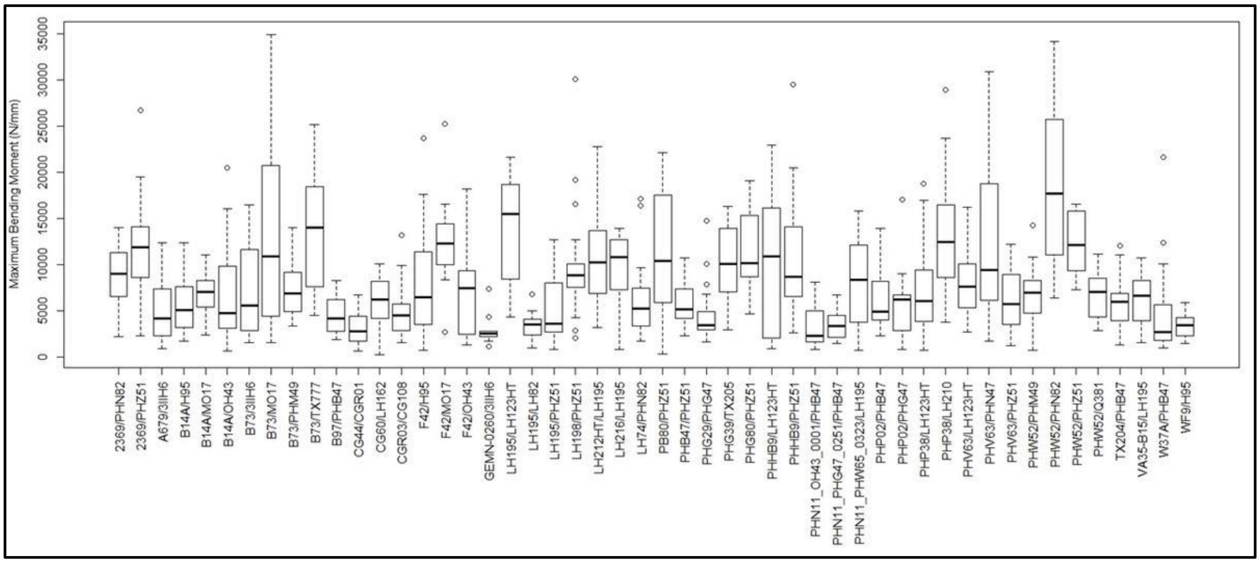

Figure 3.5: Boxplots of stalk bending strength of the Diversity Set, by hybrid.

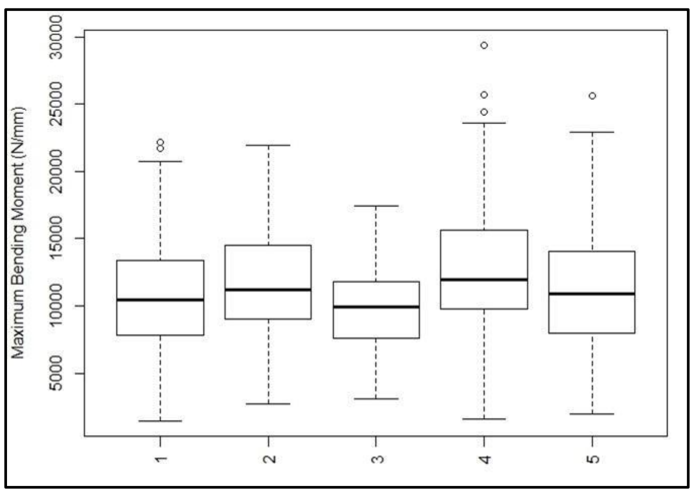

Figure 3.6: Boxplots of stalk bending strength of the Commercial Set, by hybrid.

Tables 3.2 through 3.6 summarize the findings of this analysis. In particular, these tables display the ANOVA results as obtained from the *anova* function in R; which present the usual sequential sums of squares, where p-values are for the tests that compare the models against one another in the order specified. From these results we find that hybrid type and plot are highly significant for log-strength for the Diversity Set. It should be noted that the plot variable describes the specific mesocosm, including location of planting, location within the field, and planting density. These findings indicate that there are significant genetic (i.e., hybrid type) and mesoscale (i.e. plot) effects that are still not captured with either Integrated Puncture Score or RPR. Standard model diagnostics (e.g., residual plots, QQ-plots, etc.) were conducted to assess the validity of each of these models.

	Df	Sum Sq	Mean Sq	F-statistic	P-value
Integrated Puncture Score	1	353.86	353.86	2954.647	< 2.2e-16
Hybrid	49	62.79	1.28	10.6994	< 2.2e-16
Plot	48	24.26	0.51	4.2204	< 2.2e-16
Residual	742	88.87	0.12		

Table 3.2: ANOVA analysis of Integrated Puncture Score, hybrid, and plot predicting bending strength, Diversity Set.

	Df	Sum Sq	Mean Sq	F-statistic	P-value
RPR	1	355.43	355.43	2418.795	< 2.2e-16
Hybrid	49	40.93	0.84	5.6838	< 2.2e-16
Plot	48	24.38	0.51	3.4571	4.38E-13
Residual	742	109.03	0.15		

Table 3.3: ANOVA analysis of RPR, hybrid, and plot predicting bending strength, Diversity Set.

	Df	Sum Sq	Mean Sq	F-statistic	P-value
Integrated Puncture Score	1	122.978	122.978	3682.539	< 2.2e-16
Hybrid	4	2.998	0.75	22.446	< 2.2e-16
Plot	92	12.262	0.133	3.991	< 2.2e-16

Residual	835	27.885	0.033		

Table 3.4: ANOVA analysis of Integrated Puncture Score, hybrid, and plot predicting bending strength, Commercial Set

	Df	Sum Sq	Mean Sq	F-statistic	P-value
Integrated Puncture Score	1	80.011	80.011	1271.764	< 2.2e-16
Hybrid	4	2.937	0.734	11.6703	3.16E-09
Plot	92	30.643	0.333	5.2942	< 2.2e-16
Residual	835	52.532	0.063		

Table 3.5: ANOVA analysis of RPR, hybrid, and plot predicting bending strength, Commercial Set

3.5 Discussion

Results indicate that the Integrated Puncture Score methodology provides several advantages as compared to the traditional rind penetration technique. In particular, as hypothesized, the Integrated puncture score is better able to distinguish the bending strength of elite hybrids as compared to the traditional method. One key improvement is that the Integrated Puncture Score method accounts for the cross-sectional distribution and puncture strength of various structural materials within the stalk cross-section. The traditional rind penetration method only accounts for the puncture force and is largely unaffected by gross geometric features of the stalk. However, gross geometric features are known to be principal determinants of stalk bending strength (e.g., the stalks section modulus, diameter, rind thickness etc.)[29,30]. In fact, prior research indicates that using traditional rind penetration tests as a breeding metric produces stalks with smaller diameters [7]. This is because the method does not properly account for the cross-sectional distribution of the stalks structural materials.

While the Integrated Puncture Score is a better predictor of stalk bending strength than the traditional rind penetration tests the method does have some drawbacks. For example, the Integrated Puncture Score is slightly more damaging to the plant as it requires puncturing through the entirety of the stalk cross-section as opposed to just half of the stalk cross-section. Additionally, a larger diameter probe made of high strength steel is required when utilizing the Integrated Puncture Score method to prevent the probe from bending or breaking. The method also requires collection of synchronous load-displacement data. Currently there are no field based phenotyping devices capable of collecting synchronous load-displacement data from puncture tests. The authors are currently working to develop such a device to enable Integrated Puncture Score measurements to be taken on live plants in the field. This would prevent the need to transport stalks to a laboratory for testing as was done in this study.

Several alternative approaches of analyzing the synchronous load-displacement data from a stalk puncture test were investigated as a part of this study. These included metrics such as the slope and size of different regions of the load-displacement curve, the area under different regions of the curve, and several adaptations of the Integrated Puncture Score equation. Most of these metrics were partially informed by engineering theory. However, from a structural engineering standpoint the most appropriate way in which to relate the load-displacement data from a puncture test to bending strength is by means of the Integrated Puncture Score. Indeed the predictive ability of the Integrated Puncture Score outperformed any other amalgamation of load-displacement data the authors could construe. Nonetheless to further examine the possibility of an alternative yet superior method of utilizing load-displacement data from a puncture test to predict bending strength an empirical functional regression analysis was conducted. The resulting empirical model was highly correlated ($R^2 > 0.90$) with the Integrated Puncture Score. These results suggest that neither empirical nor phenomenological relationships are more associated with the bending strength of stalks than pure engineering theory (i.e., the Integrated Puncture Score). This in turn suggests that future research should focus on improving the physical setup of puncture tests and on minimizing sources of measurement error as opposed to attempting to improve the analysis and/or post processing of puncture test data.

Several improvements may yet be realized with respect to the experimental setup of stalk puncture tests. For example, in this study a chamfered probe geometry was employed as it was shown to work well in previous studies [6,21]. However, it remains to be determined if an alternative probe geometry may provide a better relationship with stalk bending strength. In addition, the puncture rate (i.e., speed of the penetrating probe) was held constant in current study. While it is commonly accepted that the puncture rate affects test results no detailed studies have been conducted to determine what puncture rate may be most appropriate. Future studies should be careful to publish the probe geometry and puncture speed utilized in the study.

In addition, parametric analyses which simultaneously vary both puncture rate and probe geometry are needed. Because the puncture rate was held constant in the current study, it remains unclear if the Integrated Puncture Score works best by integrating the force-displacement (work) or the time-displacement (energy) data curve. In summary, the experimental setup of puncture tests should not be overlooked and should continue to be investigated and improved in the future. Previous studies into the biomechanics of stalk lodging have revealed non-intuitive confounding factors that can hamper experimental measurement efforts [31–33] and similar non-intuitive factors may affect puncture test results.

While the Integrated Puncture Score is strongly related to stalk bending strength, it should be noted that any puncture test is simply unable to simultaneously account for <u>all</u> determinants of stalk bending strength. For example, the Integrated puncture score accounts for cross-sectional distribution of structural material within the stalk but it does not account for how the material may be distributed longitudinally along the length of the stalk. Previous studies have demonstrated the importance of longitudinal tissue distribution (i.e., stalk taper) and that many genotypes exhibit structurally inefficient tapers [34]. Additionally, other studies have indicated geometric features known as stress concentrators can significantly affect stalk bending strength [29]. Neither geometric stress concentrators nor the efficiency of the stalk taper is accounted for by a single puncture test. Also of note is that puncture tests do not induce natural loading patterns on plants and therefore do not produce natural stalk lodging failure pattern in large grain crops [35]. For example, when maize plants stalk lodge they exhibit a distinct creasing failure that occurs just above the node [35,36]. The most accurate devices for phenotyping stalk lodging resistance should ideally induce natural loads and failure patterns. Additionally, results from this study indicated that genotype and environment significantly related to the bending strength of stalks even after accounting for the Integrated Puncture Score.

Limitations

Inherent to Integrated Puncture Score formulation is the assumption that the maize stem is circular and symmetrical about Point D, with a diameter equal to the measured minor diameter of the stalk. Although maize stems are elliptical, previous work has shown that the major and minor diameters are highly correlated [12]. As such, the major diameter can be reasonably approximated by the minor diameter multiplied by a constant. Substituting this into the elliptical section modulus equation causes it to reduce to the equation for the section modulus of a circle multiplied by a constant. However, constants have no effect on linear regression analyses. We therefore chose not to include the constant term in our analyses and simply utilized the equation for the section modulus of a circle when formulating Equation 2.

All puncture test methodologies used for assessing lodging resistance are based on the assumption that the plant's fracture mechanics in the transverse direction are somehow related to the tissue properties of the plant in the longitudinal direction [33]. However, a full mechanistic investigation into the exact relationship between the transverse fracture mechanics and the longitudinal elastic tissue properties of plants is required to more deeply understand the governing physics of this phenotyping approach. Such an investigation would allow researchers to better understand how parameters like probe geometry, probe speed, and stem morphology, and different plant and tissue types would affect the results, thereby enabling researchers to optimize these parameters for their specific application.

In the current study the Integrated Puncture Score was utilized to predict stalk bending strength. However, other scientists have shown that puncture tests may also be a viable manner in which to phenotype for pest and disease resistance [8,38]. Future studies should investigate the relationship between pest and disease damage (e.g., stalk rot diseases) and features of the load-displacement data curve produced during puncture tests of maize stalks.

3.6 Conclusions

The ability for plant breeders and agronomists to perform high-throughput phenotyping of stalk strength and stalk lodging resistance is still lacking. The first step in developing such a phenotyping program is to develop the testing protocol. The Integrated Puncture Score presented in this study strongly predicts stalk strength. To the best of the authors' knowledge, this is the first study to examine the entire rind penetration load-displacement curve, using the richness of the dataset to produce a physics-informed numerical score for stalk strength. Additionally, the strong agreement between the Integrated Puncture Score and the empirical model supports the claim that the presented method provides reasonable results. The Integrated Puncture Score can also differentiate between elite hybrids, potentially providing plant breeders with tools for phenotypic differentiation late in the breeding process.

Works Cited

1. Stubbs CJ, McMahan C, Seegmiller W, Cook DD, Robertson DJ. Integrated Puncture Score: Force-Displacement Weighted Rind Penetration Tests Improve Stalk Lodging Resistance Estimations in Maize.
2. Flint-Garcia SA, Jampatong C, Darrah LL, McMullen MD. Quantitative trait locus analysis of stalk strength in four maize populations. Crop Sci. 2003;43:13–22.
3. Berry P, Sylvester-Bradley R, Berry S. Ideotype design for lodging-resistant wheat. Euphytica. 2007;154:165–79.
4. Robertson DJ, Smith SL, Cook DD. On Measuring the Bending Strength of Septate Grass Stems. Am J Bot. 2015;102:5–11.
5. Berry PM, Sterling M, Spink JH, Baker CJ, Sylvester-Bradley R, Mooney SJ, et al. Understanding and Reducing Lodging in Cereals. In: Donald LS, editor. Adv Agron. Academic Press; 2004. p. 217–71.
6. Seegmiller WH, Graves J, Robertson DJ. A novel rind puncture technique to measure rind thickness and diameter in plant stalks. Plant Methods. BioMed Central; 2020;16:1–8.
7. Masole H. Evaluation of high and low divergent rind penetrometer resistance selection at three plant densities in maize. University of Missouri-Columbia; 1993.
8. Butron A, Malvar RA, Revilla P, Soengas P, Ordas A. Rind puncture resistance in maize: inheritance and relationship with resistance to pink stem borer attack. Plant Breed. 2002;121:378–82.
9. Dudley JW. Selection for Rind Puncture Resistance in Two Maize Populations. Crop Sci. 1994;34:1458–60.
10. Davis SM, Crane PL. Recurrent Selection for Rind Thickness in Maize and Its Relationship with Yield, Lodging, and Other Plant Characteristics. Crop Sci. 1976;16:53–5.
11. Jennifer Jepkurui Chesang-Chumo. Direct and correlated responses to divergent selection for rind penetrometer resistance in MoSCSS maize synthetic. [Columbia, Mo.]: University of Missouri-Columbia; 1993.
12. Kang MS, Din AK, Zhang YD, Magari R. Combining ability for rind puncture resistance in maize. Crop Sci. 1999;39:368–71.
13. Khanna KL. An improved instrument for testing rind hardness in sugarcane. Agr Live Stock India. 1935;5:156–8.

14. McRostie GP, MacLachlan JD. Hybrid corn studies I. Sci Agric. 1942;22:307–13.
15. Thompson DL. Recurrent Selection for Lodging Susceptibility and Resistance in Corn. Crop Sci. 1972;12:631–4.
16. Twumasi-Afriyie S, Hunter RB. Evaluation of quantitative methods for determining stalk quality in short-season corn genotypes. Can J Plant Sci. 1982;62:55–60.
17. Albrecht B, Dudley JW. Divergent Selection for Stalk Quality and Grain Yield in an Adapted Exotic Maize Population Cross 1. Crop Sci. Wiley Online Library; 1987;27:487–94.
18. Anderson B, White DG. Evaluation of Methods for Identification of Corn Genotypes with Stalk Rot and Lodging Resistance. Plant Dis. 1994;78:590–3.
19. Ma D, Xie R, Liu X, Niu X, Hou P, Wang K, et al. Lodging-Related Stalk Characteristics of Maize Varieties in China since the 1950s. Crop Sci. 2014;54:2805.
20. Sibale EM, Darrah LL, Zuber MS. Comparison of two rind penetrometers for measurement of stalk strength in maize. Maydica. 1992;37(1):111–4.
21. Cook DD, Meehan K, Asatiani L, Robertson DJ. The effect of probe geometry on rind puncture resistance testing of maize stalks. Plant Methods. BioMed Central; 2020;16:1–11.
22. Sekhon RS, Joyner CN, Ackerman AJ, McMahan CS, Cook DD, Robertson DJ. Stalk bending strength is strongly associated with maize stalk lodging incidence across multiple environments. 464Field Crops Res. Elsevier; 2020;249:107737.
23. Cook DD, de la Chapelle W, Lin T-C, Lee SY, Sun W, Robertson DJ. DARLING: a device for assessing resistance to lodging in grain crops. Plant Methods. 2019;15:102.
24. Robertson DJ, Julias M, Lee SY, Cook DD. Maize Stalk Lodging: Morphological Determinants of Stalk Strength. Crop Sci. 2017;57:926.
25. Stubbs CJ, Larson R, Cook DD. Mapping Spatially Distributed Material Properties in Finite Element Models of Plant Tissue Using Computed Tomography. bioRxiv. 2020
26. Stubbs CJ, Baban NS, Robertson DJ, Alzube L, Cook DD. Bending stress in plant stems: models and assumptions. Plant Biomech. Springer; 2018. p. 49–77.
27. Robertson D, Smith S, Gardunia B, Cook D.An Improved Method for Accurate Phenotyping of Corn Stalk Strength. Crop Sci. 2014;54:2038.
28. Nelson N, Stubbs CJ, Larson R, Cook DD. Measurement accuracy and uncertainty in plant biomechanics. J Exp Bot. 2019;70:3649–58.
29. Von Forell G, Robertson D, Lee SY, Cook DD. Preventing lodging in bioenergy crops: a 478biomechanical analysis of maize stalks suggests a new approach. J Exp Bot. 2015;66:7–71.

30. Stubbs CJ, Larson R, Cook DD. Maize Stem Buckling Failure is Dominated by Morphological 480Factors. BioRxiv. 2019;833863.
31. Shah DU, Schubel PJ, Licence P, Clifford MJ. Hydroxyethylcellulose surface treatment of natural fibres: the new 'twist'in yarn preparation and optimization for composites applicability. J Mater Sci. Springer; 2012;47:2700–11.
32. Al-Zube LA, Robertson DJ, Edwards JN, Sun WH, Cook DD. Measuring the compressive modulus of elasticity of pith-filled plant stems. Plant Methods. 2017;13.
33. Stubbs CJ, Sun W, Cook DD. Measuring the transverse Young's modulus of maize rind and pith tissues. J Biomech. 2019;84:113–20.
34. Stubbs CJ, Seegmiller K, Sekhon RS, Robertson DJ. Are Maize Stalks Efficiently Tapered to Withstand Wind Induced Bending Stresses? bioRxiv. 2020;
35. Robertson DJ, Julias M, Gardunia BW, Barten T, Cook DD. Corn Stalk Lodging: A Forensic Engineering Approach Provides Insights into Failure Patterns and Mechanisms. Crop Sci. 2015;55:2833.
36. Erndwein L, Cook DD, Robertson DJ, Sparks EE. Mechanical phenotyping of cereal crops to assess lodging resistance. ArXiv Prepr ArXiv190908555. 2019;
37. Gere JM, Goodno B. Mechanics of Materials. 7th ed. Florence, AL: Cengage Learning; 2008.
38. Santiago R, Souto XC, Sotelo J, Butrón A, Malvar RA. Relationship between maize stem structural characteristics and resistance to pink stem borer (Lepidoptera: Noctuidae) attack. J Econ Entomol. Oxford University Press Oxford, UK; 2003;96:1563–70.

Chapter 4 – Future Work and Conclusions

4.1 Introduction

While the Integrated Puncture Score shows promise as a breeding metric for identifying high lodging resistance breeds of maize, there is more work to be done. A portable device capable of performing the novel puncture method described in chapter 2 in a field setting must be developed. Additionally, the test procedures could be improved. This chapter presents several directions that further research into the Integrated Puncture Score could proceed.

4.2 Developing a device for field research

The Integrated Puncture Score was developed with the idea of identifying high lodging resistance maize hybrids in breeding studies. This will require the use of the Integrated Puncture Score in high throughput field measurements. The testing equipment used in this study is unsuitable for field work. Before these measurements can be used in the field, a new device must be developed.

Ideally, a device developed to determine the Integrated Puncture Score of maize stems in the field would be: handheld, light enough to use continuously for several hours, robust enough to withstand travel and exposure to dust and dirt, be tested against laboratory measurements to verify accuracy and constancy, and intuitive to use (i.e. so that field researchers can use it correctly with minimal training or technical background).

Developing a device as described above will require substantial time and effort. However, it is the natural next step in applying the Integrated Puncture Score to practical studies. By applying the Integrated Puncture Score in the field, further validation of the metric can be obtained by comparing the field measurements of the Integrated Puncture Score with the visual lodging counts of the studied plots over time. Then the Integrated Puncture Score can be confidently used as a predictive measure of maize lodging resistance.

4.3 Improving the testing method

The Integrated puncture score is highly correlated with the empirical model presented in chapter 3. This suggests that the Integrated Puncture Score extracts most of the data pertinent to the lodging resistance of a sample from its associated load-displacement curve. While this affirms the accuracy of the Integrated Puncture Score as generated from the load displacement curve, there are possible ways that the load displacement curve itself might be enhanced by improving our test equipment and procedures. The following paragraphs detail several possible ways to enhance the rind puncture method.

Determining the optimal probe tip geometry

In a puncture test, probe geometry has a strong effect on the quality of the results. Before collecting data for this study, exploratory tests on several probe geometries (i.e. sharp probes, flat tipped probes, and chamfered probes) were carried out. The chamfered probe was selected for use due to its advantages over the others as presented in the following paragraphs. However, it is unclear if this probe geometry is the most optimal for rind puncture tests. Determining the optimal probe geometry for rind puncture tests is difficult because optimal probe geometry is dependent on many interrelated factors and is possibly species dependent. The following paragraphs present the results of the exploratory tests and the reasoning by which the selected probe geometry was chosen.

Probe with sharp tipped end condition

Figure 4.1 shows the results of a puncture test carried out with a sharp probe. The sharp probe slides between the fibrous elements of the stem, and subsequently displaces stem tissues perpendicularly to the probe axis of travel. This causes the displaced tissues to exert a strong compressive force on the surface of the probe as it punctures through the stem. The data obtained by this method does indicate a diameter and rind thickness but is very hard to analyze algorithmically. Additionally, the probe does not interact with both the fibrous and connective tissues in the rind, and therefore does not give any indication of the bulk properties of the rind tissue. These disadvantages disqualified sharp tipped probes for use in the current study.

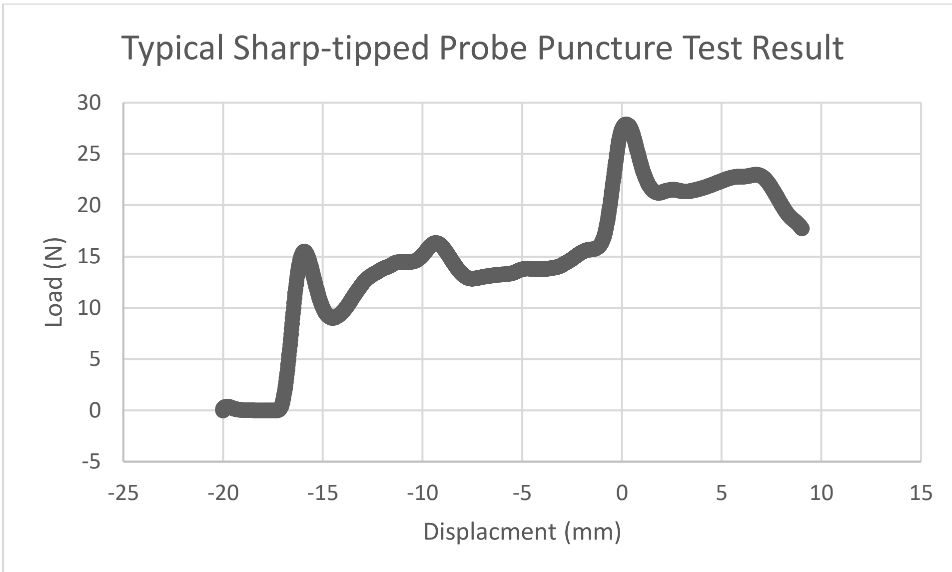

Figure 4.1: Sharp tipped probes are not recommended for the novel puncture method due to the difficulty of analyzing the resulting curve and the large friction effects.

Probe with flat tipped end condition

Figure 4.2 shows the results of a puncture test carried out with a flat tipped probe. The probe simultaneously interacts with fibrous and connective tissues in the rind as it punctures the stem. This results in a void in the rind tissue. Therefore, the flat tipped probe experiences much less frictional resistance than the sharp tipped probe throughout the test. The data obtained by the flat tipped probe is relatively easy to analyze algorithmically, and the shape of the graphed data corresponds to the material organization of the stem cross section. However, the flat tipped probe tends to skate along the rounded, uppermost surface of the stem being measured for between one to three millimeters (i.e. the tip of the probe would bend one to three millimeters away from its horizontal orientation) before finally puncturing through the surface of the material. This results in the tip of the probe taking a nonlinear path through the tissue. Determinations of rind thickness and diameter from such tests exhibit a large degree of error. In some of these tests, the probe is permanently deformed as a result of this phenomenon. Additionally, Figure 4.3 shows how the flat tipped probe may have large error in rind thickness measurements. Because of the interaction of the relatively wide probe surface and the concave surface of the inner rind, a flat tipped probe will tend to overpredict the rind thickness of samples. This effect is more marked for smaller diameter specimens. These disadvantages disqualified flat tipped probes for use in the current study.

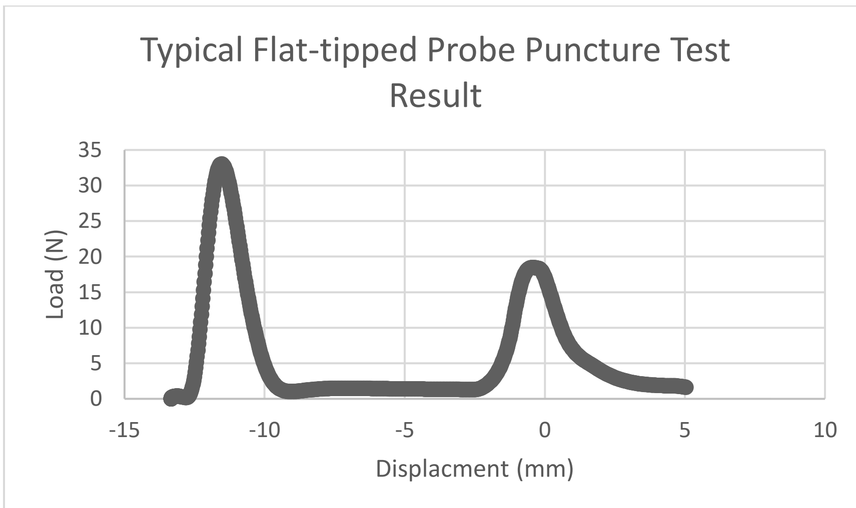

Figure 4.2: Flat tipped probes reliably produce an easy to analyze curve, but do not outperform the chamfered-tipped probes.

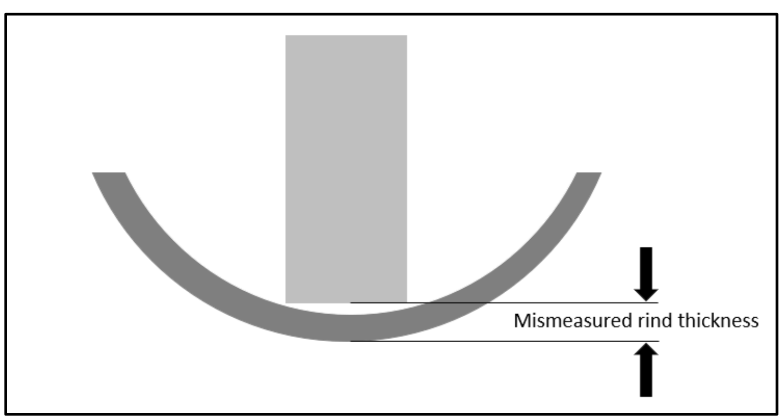

Figure 4.3: This diagram presents the cause of the consistent overprediction of the rind thickness by a flat tipped probe. The scale of this diagram has been altered to more clearly present the geometrical interactions of probe and rind.

Probe with chamfered end condition

All puncture data collected for this study was obtained using a chamfered probe. In nearly all considerations, it behaves like flat tipped probe, but it does not have the same tendency to skate along the stem surface because the leading surface a has smaller area than the flat tipped probe. Additionally, chamfered probes do not tend to overpredict rind thickness as a flat tipped probe would due to the lower area of the leading surface. These advantages lead to the selection of chamfered tipped probes for the current study.

Determining optimal probe size

In general, a probe intended to puncture maize or sorghum should be between 1 to 2.5 millimeters in diameter. This scale allows the probe to interact with between 2-5 major fibers as it punctures through the rind. This is important because without major fiber interactions, the probe will not experience the true puncture resistance of the rind. This scale is also small enough that the entire leading surface of the probe will impact the rind at approximately the same instant.

The larger a probe is, the stiffer it will be. In exploratory tests, it was determined that maximizing the stiffness of the probe is desirable to reduce the probability of deflection occurring as the probe leading surface makes initial contact with the rounded surface of the sample. Therefore, a probe should be made from the stiffest available materials and should have as large a diameter as possible without sacrificing effectiveness (i.e. without being so large that the leading surface does not impact the rind all at once).

Determining optimal probe travel rate

One factor that complicates many studies of biological tissues is that biological tissues exhibit viscoelastic properties. This suggests that the puncture test used to determine the Integrated Puncture Score of a maize sample could produce varied results based on the rate of travel of the probe. Further study is required to determine the significance of the effect of the rate of travel of the probe. If the effect is significant, the optimal range of probe travel rates for calculating the Integrated Puncture Score should be determined.

Determining the optimal range of instrument sample rates

While the 1000hz sample rate of the instruments used in this study provides good resolution data for analysis, a study into the effects of sample rate on Integrated Puncture Score accuracy may provide interesting results. Determining the upper threshold of instrument sample rate that produces incremental gains in Integrated Puncture Score accuracy and the lower threshold of instrument sample rate that produces an accurate calculation of the Integrated Puncture Score may be useful. This information could be used to inform the development of field ready devices to ensure that field measurements are valid.

Study of lodging resistance in other plant species

Many other plants that are grown on an industrial scale could benefit from a lodging resistance measurement like the Integrated Puncture Score (e.g. sorghum, bamboo, sugar cane, etc.). Further research is needed to determine how the Integrated Puncture Score could be applied to other species. Certain alterations to the calculation of the Integrated Puncture Score may be required to account for unique plant species geometry and structure.

4.4 Conclusions

The Integrated Puncture Score has been shown to be effective at predicting the lodging resistance of maize samples in laboratory settings. Further development is needed to bring this technology to the field for further testing, and so that it may be utilized for its intended purpose (i.e. to allow maize studies and breeding programs to identify lodging resistance strains of maize). Further research may lead to improvements in testing procedures and equipment. The Integrated Puncture Score may be expanded to predict lodging resistance in other plant species with further study.